

## Responses to Editor's comments:

This manuscript is a re-submission, based on a previous manuscript (<https://www.hydrol-earth-syst-sci-discuss.net/hess-2016-624/>). The 3 reviewers are relatively satisfied with the revised manuscript, and all recommend minor revision. The authors' responses indicate that they accept the reviewer comments, and indeed the authors have already submitted a revised manuscript addressing all reviewer comments.

I am generally satisfied with the manuscript and the authors' responses to the review comments. I have two editorial suggestions:

**Thanks for the invaluable suggestions. We have revised the manuscript accordingly (please see the point-to-point responses below).**

1. A statement to the effect that "Increased P, ET and Q were found in most TP basins during the past 30 years except for the upper Yellow River basin and some sub-basins of Yalong River," appears in several places in the manuscript. I think it needs to be qualified because few of the increases were shown to be statistically significant. The fact that so many of the trend slopes are positive is certainly suggestive of an overall increase, but either more argument is needed to make this point, or additional qualification should be added.

Here I summarise the number of statistically significant increases shown in Figs 8, 10, 11

Westerly-dominated: Fig 8: P 0/3 ; ETwb 0/3; Q 1/3

East-Asian monsoon Fig 10: P 1/9 ; ETwb 3/9; Q 0/9

Indian monsoon Fig 11: P 2/6 ; ETwb 4/6; Q 1/6

Total over all basins: P 3/18; ETwb 7/18; Q 2/18

In total, 12 out of these 54 variables show a statistically significant increase.

**We totally agree with you. In the revised version, we have added more additional qualifications to the expressions of results related to the trends, using more precise words (i.e., significant/insignificant, markedly/slightly, distinctly/marginally). We are sure that the improved expressions (please see the revisions in Section 3.3 and the related parts in Summary and Abstract) can be more accurate and clear to readers. Thank you very much.**

2. The presentation of the 18 basins in Tables 2,3,4 would be improved if they were separated into the 3 sub-groups used elsewhere in the manuscript.

**Done! Thanks. Please see the revised Tables R1-R3 (Tables 2, 3 and 4 in the new version) in the following pages in this file.**

**Table R1: Main features of the 18 TP river basins used in this study. The precipitation and temperature statistics for each basin were calculated from the observed CMA datasets while the NDVI and LAI statistics were extracted from the GIMMS NDVI dataset and GLASS LAI product. The GA% and SC% represented the percentages of multiyear-mean glacier cover and snow cover in each basin which were calculated from the Second Glacier Inventory Dataset of China and the daily TP snow cover dataset (2005-2013)**

| No.  | Station       | Altitude<br>(m) | River name  | Drainage area<br>(km <sup>2</sup> ) | Multiyear-mean (1982-2011) and basin-averaged parameters |               |                           |      |      |       |       |
|--|---------------|-----------------|-------------|-------------------------------------|--|---------------|---------------------------|------|------|-------|-------|
|  |               |                 |             |                                     | Q (mm/yr)  | Prec. (mm/yr) | Temp.( <sup>o</sup> C/yr) | NDVI | LAI  | GA%   | SC%   |
| <i><b>Westerlies-dominated basins:</b></i>         |               |                 |             |                                     |  |               |                           |      |      |       |       |
| 01   | Kulukelangan  | 2000            | Yerqiang    | 32880.00                            | 158.60   | 128.34        | -5.68                     | 0.05 | 0.03 | 10.97 | 35.03 |
| 02   | Tongguziluoke | 1650            | Yulongkashi | 14575.00                            | 151.56   | 134.04        | -4.07                     | 0.06 | 0.04 | 23.27 | 35.95 |
| 03   | Numaitilangan | 1880            | Keliya      | 7358.00                             | 103.18   | 137.14        | -4.78                     | 0.06 | 0.03 | 10.86 | 29.16 |
| <i><b>East Asian monsoon-dominated basins:</b></i> |               |                 |             |                                     |  |               |                           |      |      |       |       |
| 04   | Zelingou      | 4282            | Bayin       | 5544.00                             | 41.42  | 340.68        | -4.98                     | 0.13 | 0.09 | 0.09  | 21.22 |
| 05   | Gadatan       | 3823            | Yellow      | 7893.00                             | 200.95   | 566.01        | -4.60                     | 0.34 | 0.54 | 0.13  | 14.94 |
| 06   | Xining        | 3225            | Yellow      | 9022.00                             | 99.90  | 503.74        | 0.97                      | 0.36 | 0.70 | 0.00  | 10.06 |
| 07   | Tongren       | 3697            | Yellow      | 2832.00                             | 149.36   | 533.25        | -1.37                     | 0.39 | 0.83 | 0.00  | 9.42  |
| 08   | Tainaihai     | 2632            | Yellow      | 121972.00                           | 159.48   | 540.32        | -2.40                     | 0.34 | 0.72 | 0.09  | 15.89 |
| 09   | Huangheyan    | 4491            | Yellow      | 20930.00                            | 31.18  | 386.42        | -4.81                     | 0.23 | 0.61 | 0.00  | 17.25 |
| 10   | Jimai         | 4450            | Yellow      | 45015.00                            | 85.50  | 441.48        | -4.16                     | 0.26 | 0.52 | 0.00  | 20.05 |
| 11   | Yajiang       | 2599            | Yalong      | 67514.00                            | 237.66   | 717.05        | -0.23                     | 0.43 | 0.80 | 0.15  | 18.36 |
| 12   | Zhimenda      | 3540            | Yangtze     | 137704.00                           | 96.23  | 405.66        | -4.83                     | 0.20 | 0.26 | 0.96  | 17.87 |
| <i><b>Indian monsoon-dominated basins:</b></i>     |               |                 |             |                                     |  |               |                           |      |      |       |       |
| 13   | Jiaoyuqiao    | 3000            | Salween     | 72844.00                            | 364.26   | 620.88        | -1.89                     | 0.29 | 0.44 | 2.02  | 23.73 |
| 14   | Pangduo       | 5015            | Brahmaputra | 16459.00                            | 348.31   | 544.59        | -1.53                     | 0.27 | 0.33 | 1.66  | 23.33 |
| 15   | Tangjia       | 4982            | Brahmaputra | 20143.00                            | 350.61   | 555.17        | -1.89                     | 0.27 | 0.34 | 1.39  | 21.83 |

|    |               |      |             |           |        |        |       |      |      |      |       |
|----|---------------|------|-------------|-----------|--------|--------|-------|------|------|------|-------|
| 16 | Gongbujiangda | 4927 | Brahmaputra | 6417.00   | 586.96 | 692.06 | -4.24 | 0.27 | 0.36 | 4.12 | 25.99 |
| 17 | Nuxia         | 2910 | Brahmaputra | 191235.00 | 307.38 | 401.35 | -0.73 | 0.22 | 0.25 | 1.90 | 13.50 |
| 18 | Yangcun       | 3600 | Brahmaputra | 152701.00 | 163.25 | 349.91 | -0.87 | 0.19 | 0.18 | 1.28 | 10.52 |

---

**Table R2: Annual-averaged water storage changes ( $\Delta S$ ) in 18 TP basins derived from GRACE retrievals (2002-2013) from three different processing centers (CSR, GFZ and JPL)**

| Basin  | Water storage Change ( $\Delta S$ ,mm) |       |       |
|--|--|-------|-------|
|  | CSR                                    | GFZ   | JPL   |
| <b><i>Westerlies-dominated basins:</i></b>         |  |       |       |
| Kulukelangan                                       | -0.16                                  | -0.16 | -0.00 |
| Tongguziluoke                                      | 0.10                                   | 0.10  | 0.28  |
| Numaitilangan                                      | 0.24                                   | 0.22  | 0.41  |
| <b><i>East Asian monsoon-dominated basins:</i></b> |  |       |       |
| Zelingou   | 0.63                                   | 0.41  | 0.69  |
| Gadatan  | 0.02                                   | -0.24 | -0.03 |
| Xining   | -0.08                                  | -0.35 | -0.14 |
| Tongren  | -0.13                                  | -0.41 | -0.21 |
| Tainaihai  | 0.12                                   | -0.16 | 0.10  |
| Huangheyan   | 0.60                                   | 0.35  | 0.70  |
| Jimai  | 0.41                                   | 0.15  | 0.48  |
| Yajiang  | -0.23                                  | -0.50 | -0.21 |
| Zhimenda   | 0.57                                   | 0.38  | 0.78  |
| <b><i>Indian monsoon-dominated basins:</i></b>     |  |       |       |
| Jiaoyuqiao   | -1.00                                  | -1.13 | -0.79 |
| Nuxia  | -1.42                                  | -1.44 | -1.31 |
| Pangduo  | -1.21                                  | -1.29 | -1.02 |
| Tangjia  | -1.40                                  | -1.46 | -1.24 |
| Gongbujiangda                                      | -1.61                                  | -1.67 | -1.47 |
| Yangcun  | -1.33                                  | -1.34 | -1.21 |

**Table R3: Nonparametric trends for different ET estimates during the period 1982-2006 detected by modified Mann-Kendall test, the bold number showed the detected trend is statistically significant at the 0.05 level**

| Basin  | ET <sub>wb</sub> | GLEAM_E     | VIC_E       | Zhang_E      | PML_E       | MET_E        | GNoah_E     |
|--|------------------|-------------|-------------|--------------|-------------|--------------|-------------|
| <b><i>Westerlies-dominated basins:</i></b>         |                  |             |             |              |             |              |             |
| Kulukelangan                                       | <b>-0.09</b>     | 0.09        | <b>0.18</b> | —            | 0.03        | -0.01        | 0.07        |
| Tongguziluke                                       | -0.02            | 0.10        | <b>0.13</b> | —            | 0.03        | <b>-0.08</b> | 0.19        |
| Numaitilangan                                      | 0.04             | <b>0.10</b> | 0.14        | —            | 0.14        | <b>-0.10</b> | 0.22        |
| <b><i>East Asian monsoon-dominated basins:</i></b> |                  |             |             |              |             |              |             |
| Zelingou   | <b>0.13</b>      | <b>0.23</b> | 0.11        | <b>0.09</b>  | 0.04        | <b>0.06</b>  | 0.02        |
| Gadatan  | -0.09            | 0.25        | 0.070       | -0.10        | -0.01       | <b>0.06</b>  | -0.07       |
| Xining   | -0.06            | <b>0.54</b> | 0.01        | -0.08        | 0.01        | 0.02         | -0.06       |
| Tongren  | -0.06            | <b>0.34</b> | -0.15       | <b>-0.17</b> | 0.07        | 0.02         | 0.13        |
| Tainaihai  | 0.06             | <b>0.28</b> | -0.03       | <b>-0.11</b> | 0.04        | <b>0.05</b>  | 0.04        |
| Huangheyan   | 0.08             | <b>0.19</b> | -0.01       | <b>-0.10</b> | <b>0.08</b> | <b>0.05</b>  | <b>0.10</b> |
| Jimai  | -0.07            | <b>0.23</b> | -0.01       | -0.08        | 0.03        | <b>0.05</b>  | 0.10        |
| Yajiang  | 0.17             | <b>0.26</b> | <b>0.06</b> | <b>-0.21</b> | -0.01       | 0.03         | -0.02       |
| Zhimenda   | 0.11             | <b>0.28</b> | 0.10        | 0.01         | 0.07        | <b>0.04</b>  | 0.07        |
| <b><i>Indian monsoon-dominated basins:</i></b>     |                  |             |             |              |             |              |             |
| Jiaoyuqiao   | <b>0.18</b>      | <b>0.28</b> | 0.10        | <b>-0.11</b> | 0.05        | <b>0.05</b>  | 0.07        |
| Nuxia  | <b>-0.09</b>     | <b>0.25</b> | 0.09        | <b>-0.10</b> | <b>0.12</b> | <b>0.04</b>  | 0.10        |
| Pangduo  | 0.05             | <b>0.28</b> | <b>0.17</b> | <b>-0.07</b> | 0.07        | <b>0.07</b>  | <b>0.11</b> |
| Tangjia  | 0.09             | <b>0.26</b> | <b>0.17</b> | <b>-0.09</b> | <b>0.20</b> | <b>0.06</b>  | <b>0.12</b> |
| Gongbujiangda                                      | -0.26            | 0.12        | 0.13        | <b>-0.16</b> | <b>0.19</b> | 0.01         | <b>0.15</b> |
| Yangcun  | 0.03             | <b>0.28</b> | 0.08        | <b>-0.06</b> | 0.10        | 0.04         | 0.09        |



**Investigating water budget dynamics in 18 river basins across Tibetan Plateau through multiple datasets**

Wenbin Liu<sup>a</sup>, Fubao Sun<sup>a,b,h,i\*</sup>, Yanzhong ~~Li~~<sup>a</sup>Li<sup>c</sup>, Guoqing ~~Zhang~~<sup>e</sup>Zhang<sup>d,de</sup>, Yan-Fang Sang<sup>a</sup>,  
Wee Ho Lim<sup>a,ef</sup>, Jiahong ~~Li~~<sup>f</sup>Liu<sup>g</sup>, Hong Wang<sup>a</sup>, Peng Bai<sup>a</sup>

<sup>a</sup>Key Laboratory of Water Cycle and Related Land Surface Processes, Institute of Geographic Sciences and Natural Resources Research, Chinese Academy of Sciences, Beijing 100101, China

<sup>b</sup>Hexi University, Zhangye 734000, China

<sup>c</sup>College of Hydrometeorology, Nanjing University of Information Science and Technology, Nanjing 210044, China

<sup>d,e</sup>Key Laboratory of Tibetan Environmental Changes and Land Surface Processes, Institute of Tibetan Plateau Research, Chinese Academy of Sciences, Beijing 100101, China

<sup>d,e</sup>CAS Center for Excellent in Tibetan Plateau Earth Sciences, Beijing 100101, China

<sup>e,f</sup>Environmental Change Institute, Oxford University Centre for the Environment, School of Geography and the Environment, University of Oxford , Oxford OX1 3QY, UK

<sup>f,g</sup>Key Laboratory of Simulation and Regulation of Water Cycle in River Basin, China Institute of Water Resources and Hydropower Research, Beijing 100038, China

<sup>h</sup>College of Resources and Environment, University of Chinese Academy of Sciences, Beijing 100049, China

<sup>i</sup>Center for Water Resources Research, Chinese Academy of Sciences, Beijing 100101, China

带格式的: 缩进: 左侧: 0 厘米, 悬挂缩进: 0.5 字符, 首行缩进: -0.5 字符

带格式的: 缩进: 左侧: 0 厘米, 悬挂缩进: 0.5 字符, 首行缩进: -0.5 字符

27 |  
28 **Re-submitted to:** Hydrology and Earth System Sciences  
29 **Corresponding Author:** Dr. Fubao Sun ([Sunfb@igsnr.ac.cn](mailto:Sunfb@igsnr.ac.cn)), Key Laboratory of Water Cycle  
30 and Related Land Surface Processes, Institute of Geographic Sciences and Natural Resources  
31 Research, Chinese Academy of Sciences  
32 |  
33 2017/~~40~~11



**Abstract** The dynamics of basin-scale water budgets are not well understood nowadays over the Tibetan Plateau (TP) due to the lack of in situ hydro-climatic observations. In this study, we investigate the seasonal cycles and trends of water budget components (e.g., precipitation-P, evapotranspiration-ET and runoff-Q) in eighteen TP river basins during the period 1982-2011 through the use of multi-source datasets (e.g., in situ observations, satellite retrievals, reanalysis outputs and land surface model simulations). A water balance-based two-step procedure, which considers the changes in basin-scale water storage at the annual scale, is also adopted to calculate actual ET. The results indicated that precipitation (mainly snowfall from mid-autumn to next spring), which mainly concentrated during June-October (varied among different monsoons-impacted basins), was the major contributor to the runoff in TP basins. ~~Increased~~ The P, ET and Q were found marginally increase in most TP basins during the past 30 years except for the upper Yellow River basin and some sub-basins of Yalong River, which were mainly affected by the weakening East Asian Monsoon. Moreover, the aridity index (PET/P) and runoff coefficient (Q/P) slightly decreased in most basins, which were in agreement with the warming and moistening climate in the Tibetan Plateau. The results obtained demonstrated the usefulness of integrating multi-source datasets to hydrological applications in the data-sparse regions. More generally, such approach might offer helpful insights towards understanding the water and energy budgets and sustainability of water resource management practices of data-sparse regions in a changing environment.

## 1 Introduction

As the highest plateau in the globe (the average elevation is higher than 4000 meters above the sea level), the Tibetan Plateau (TP, also called “the roof of the world” or “the third Pole”) is regarded as one of the most vulnerable regions under a warming climate and is exposed to strong interactions among atmosphere, hydrosphere, biosphere and cryosphere in the earth system (Duan and Wu, 2006; Yao et al., 2012; Liu et al., 2016b). It also serves as the “Asian water tower” from which some major Asian rivers such as Yellow River, Yangtze River, Brahmaputra River, Mekong River, Indus River, etc., originate, which is a vital water resource to support the livelihood of hundreds of millions of people in China and the neighboring Asian countries (Immerzeel et al., 2010; Zhang et al., 2013). Hence sound knowledge of water budget and hydrological regimes in TP river basins and their responses to the changing environment would have practical relevance for achieving sustainable water resource management and environmental protection in this part of the world (Yang et al., 2014; Chen et al., 2015).

Despite the importance of TP in this geographic region, advance in hydrological and land surfaces studies in this region has been limited by data scarcity (Zhang et al., 2007; Li F. et al., 2013; Liu X. et al., 2016). For instance, less than 80 observation stations (~10% of a total of ~750 observation station across China) have been established in TP by the Chinese Meteorological Administration (CMA) since the mid-20<sup>th</sup> century (Wang and Zeng, 2012). These stations are generally sparse and unevenly distributed at relatively low elevation regions (most stations are located in the eastern TP and few of them situated in the western parts), focus only on the meteorological variables and lack of other land surface observations such as

81 evapotranspiration, snow water equivalent and latent heat fluxes. In addition,  
82 long-term observations of river discharge, lake depth and glacier melts in the TP are  
83 also absent (Akhta et al., 2009; Ma et al., 2016). Therefore, the water budget and  
84 hydrological regimes for each river basin of TP and their relation with atmospheric  
85 circulations are poorly understood (Cuo et al., 2014; Xu et al., 2016). Whilst this  
86 shortcoming could be resolved through installation of in-situ monitoring systems  
87 (Yang et al., 2013; Zhou et al., 2013; Ma et al., 2015), the overall cost, labor and  
88 technical support for running the operational sites would be substantial. Another  
89 workaround would be through modeling approach, i.e., feeding remote sensing  
90 information and meteorological forcing data into physically-based land surface model  
91 (LSM) to simulate the basin-wide water budget (Bookhagen and Burbank, 2010; Xue  
92 et al., 2013; Zhang et al., 2013; Cuo et al., 2015; Zhou et al., 2015; Wang et al., 2016).  
93 However, such approach is not immune from the issue of data scarcity at multiple  
94 river basins (with varied sizes and/or terrain complexities) for supporting model  
95 calibration and validation purposes (Li F. et al., 2014).

96  
97 Most recently, several global (or regional) datasets relevant to the calculation of water  
98 budget have been released. They include remote sensing-based retrievals (Tapley et al.,  
99 2004; Zhang et al., 2010; Long et al., 2014; Zhang Y. et al., 2016), land surface model  
100 (LSM) simulations (Rui, 2011), reanalysis outputs (Berrisford et al., 2011; Kobayashi  
101 et al., 2015) and gridded forcing data interpolated from the in situ observations  
102 (Harris et al., 2014). For example, there are many products related to terrestrial  
103 evapotranspiration (ET) such as GLEAM\_E (Global Land surface Evaporation: the  
104 Amsterdam Methodology, Miralles et al., 2011a), MTE\_E (a product integrated the  
105 point-wise ET observation at FLUXNET sites with geospatial information extracted

from surface meteorological observations and remote sensing in a machine-learning algorithm, Jung et al., 2010 ), LSM-simulated ETs from Global Land Data Assimilation System version 2 (GLDAS-2) with different land surface schemes (Rodell et al., 2004), ETs from Japanese 55-year reanalysis (JRA55\_E), the ERA-Interim global atmospheric reanalysis dataset (ERA-Interim) and the National Aeronautic and Space Administration (NASA) Modern Era Retrospective-analysis for Research and Application (MERRA) reanalysis data (Lucchesi, 2012). Moreover, there are also several global or regional LSM-based runoff simulations from GLDAS and the Variable Infiltration Capacity (VIC) model (Zhang et al., 2014). A few attempts have been made to validate multiple datasets for certain water budget components and to explore their possible hydrological implications. For example, Li X. et al. (2014) and Liu et al. (2016a) evaluated multiple ET estimates against the water balance method at annual and monthly time scales. Bai et al. (2016) assessed streamflow simulations of GLDAS LSMs in five major rivers over the TP based on the discharge observations. Although uncertainties might exist among different datasets with various spatial and temporal resolutions and calculated using different algorithms (Xia et al., 2012), they offer an opportunity to examine the general basin-wide water budgets and their uncertainties in gauge-sparse regions such as the TP considered in this study.

From the multiple datasets perspective, this study aims to investigate the water budget in 18 TP river basins distributed across the Tibetan Plateau; and evaluate seasonal cycles and annual trends of these water budget components. This paper is organized as follows: the datasets and methods applied in this study are described in Sect.2. The results of season cycles and annual trends of water budget components for the river

basins are presented and discussed in Sect.3. The uncertainties arise from employing multiple datasets are also discussed in the same section. In Sect.4, we generalize our findings which would be helpful for understanding the water balances of the river basins under constant influence of interplay between westerlies and monsoons (e.g., Indian monsoon, East Asian monsoon) in the Tibetan Plateau.

## **2 Data and methods**

### **2.1 Multiple datasets used**

#### **2.1.1 Runoff, precipitation and terrestrial storage change**

We obtained the observed daily runoff ( $Q$ ) during the period 1982-2011 from the National Hydrology Almanac of China (Table 1). There are < 30% missing data in some gauging stations such as Yajiang, Tongren, Gandatan and Zelingou. Therefore, the VIC Retrospective Land Surface Dataset over China (1952-2012, VIC\_IGSNRR simulated) with a spatial resolution of 0.25 degree and a daily temporal resolution from the Geographic Sciences and Natural Resources Research (IGSNRR), Chinese Academy of Sciences, is also used. This dataset is derived from the VIC model forced by the gridded daily observed meteorological forcing (IGSNRR\_forcing) (Zhang et al., 2014). A degree-day scheme was used in the model to account for the influences of snow and glacier on hydrological processes.

In terms of precipitation ( $P$ ), we used the gridded monthly precipitation dataset available at CMA (spatial resolution of 0.5 degree; 1961-2011; interpolated from observations of 2372 national meteorological stations using the Thin Plate Spline method) (Table 1). Since the reliability of this dataset might be restricted by the relatively sparse stations and complex terrain conditions of TP, we make an attempt to

incorporate two other precipitation datasets ((IGSNRR\_forcing and Tropical Rainfall Measuring Mission TRMM 3B43 V7). The precipitation from IGSNRR forcing datasets (0.25 degree) was derived by interpolating gauged daily precipitation from 756 CMA stations based on the synergraphic mapping system algorithm (Shepard, 1984; Zhang et al., 2014) and was further bias-corrected using the CMA gridded precipitation.

<Table 1, here please, thanks>

带格式的: 字体颜色: 自动设置

To get the change in terrestrial storage ( $\Delta S$ ), we used three latest global terrestrial water storage anomaly and water storage change datasets (available on the GRACE Tellus website: <http://grace.jpl.nasa.gov/>) that were retrieved from the Gravity Recovery and Climate Experiment (GRACE, Tapley et al., 2004; Landerer and Swenson, 2012; Long et al., 2014). Briefly, they were processed separately at the Jet Propulsion Laboratory (JPL), the GeoForschungsZentrum (GFZ) and the Center for Space Research at the University of Texas (CSR). To minimize the errors and uncertainty of extracted  $\Delta S$ , we averaged these GRACE retrievals (2002-2013) from different processing centers in this study.

### 2.1.2 Temperature, potential evaporation and ET

We obtained the monthly gridded temperature dataset (0.5 degree) from CMA; and potential evaporation (PET) dataset (0.5 degree, Harris et al., 2013) from Climatic Research Unit (CRU), University of East Anglia. Moreover, we used six global /regional ET products (four diagnostic products and two LSMs simulations, Table 1), namely (1) GLEAM\_E (Miralles et al., 2010, 2011), which consists of three sources of ET (transpiration, soil evaporation and interception) for bare soil, short vegetation

and vegetation with a tall canopy calculated using a set of algorithm ([www.gleam.eu](http://www.gleam.eu)),  
 (2) GNoah\_E simulated using GLDAS-2 with the Catchment Noah scheme  
 (<http://disc.sci.gsfc.nasa.gov/hydrology/data-holdings>) (Rodell et al., 2004), (3)  
 Zhang\_E (Zhang et al., 2010), which is estimated using the modified  
 Penman-Monteith equation forced with MODIS data, satellite-based vegetation  
 parameters and meteorological observations (<http://www.nts.gov/project/et>), (4)  
 MET\_E (Jung et al., 2010) (<https://www.bgc-jena.mpg.de/geodb/projects/Home.phs>),  
 (5) VIC\_E (Zhang et al., 2014) from VIC\_IGSNRR simulations  
 ([http://hydro.igsnrr.ac.cn/public/vic\\_outputs.html](http://hydro.igsnrr.ac.cn/public/vic_outputs.html)) and (6) PML\_E (Zhang Y. et al.,  
 2016) computed from global observation-driven Penman-Monteith-Leuning (PML)  
 model (<https://data.csiro.au/dap/landingpage?pid=csiro:17375&v=2&d=true>).

### 2.1.3 Vegetation and snow/glacier parameters

To quantify the dynamics of vegetation of each river basin, we applied the  
 Normalized Difference Vegetation Index (NDVI) and the Leaf Area Index (LAI)  
 (Table 1). Briefly, the NDVI data was obtained from the Global Inventory Modeling  
 and Mapping Studies (GIMMS) (Turker et al., 2005)  
 ([https://nex.nasa.gov/nex/projects/1349/wiki/general\\_data\\_description\\_and\\_access/](https://nex.nasa.gov/nex/projects/1349/wiki/general_data_description_and_access/))  
 while the LAI data was collected from the Global Land Surface Satellite (GLASS)  
 products (<http://www.glcfc.umd.edu/data/lai/>) (Liang and Xiao, 2012). Whist the  
 change in seasonal snow cover and glacier has significant impact on the water and  
 energy budgets in TP river basins; it remains a technical challenge to get reliable  
 observations due to harsh environment (especially at the basin scale). However,  
 recently available satellite-based/LSM-simulated products might provide adequate

characterization of the variation of snow cover and glacier. To quantify the change in snow cover at each basin, we applied the daily cloud free snow composite product from MODIS Terra-Aqua and the Interactive Multisensor Snow and Ice Mapping System for the Tibetan Plateau (Zhang et al., 2012; Yu et al., 2015), in conjunction with the snow water equivalent (SWE) retrieved from Global Snow Monitoring for Climate Research product (GlobSnow-2, <http://www.globsnow.info/>) and the VIC\_IGSNRR simulations (Takala et al., 2011; Zhang et al., 2014). We extracted general distribution of glacier of TP from the Second Glacier Inventory Dataset of China (Guo et al., 2014). All gridded datasets used were first uniformly interpolated to a spatial resolution of 0.5 degree based on the bilinear interpolation to make their inter-comparison possible. The datasets were then extracted for each of TP basins.

#### **2.1.4 Monsoon indices**

In general, the TP climate is under the influences of the westerlies, Indian summer monsoon and East Asian summer monsoon (Yao et al., 2012). To investigate the changes of monsoon systems and their potential impacts on water budgets in the TP basins, we used three monsoon indices, namely Asian Zonal Circulation Index (AZCI), Indian Ocean Dipole Mode Index (IODMI) and East Asian Summer Monsoon Index (EASMI). Briefly, the IODMI (reflects the dynamics of Indian Summer Monsoon) is an indicator of the east-west temperature gradient across the tropical Indian Ocean (Saji et al., 1999), which can be downloaded from the following website: <http://www.jamstec.go.jp/frcgc/research/d1/iod/HTML/Dipole%20Mode%20Index.html>. The EASMI and AZCI (60°-150°E) reflect the dynamics of East Asian summer monsoon (Li and Zeng, 2002) and the westerlies (represented by Asian Zonal Circulation index), which can be obtained from Beijing Normal University



(<http://ljp.gcess.cn/dct/page/65577>) and the National Climate Center of China  
(<http://ncc.cma.gov.cn/Website/index.php?ChannelID=43WCHID=5>), respectively.

**2.1.5 Study basins**

In this study, we selected 18 river basins of varied sizes (range: 2832-191235 km<sup>2</sup>; see Table 2 for details) with adequate runoff data over a 30-year period (1982-2011). They are distributed in the northwestern, southeastern and eastern parts of the plateau with multiyear-mean and basin-averaged temperature and precipitation ranging from -5.68 to 0.97 °C and 128 to 717 mm, which are solely dominated or under the combined influences of the westerlies, the Indian Summer monsoon and the East Asian monsoon (Yao et al., 2012). There are more glacier and snow covers in the westerlies-dominant basins such as Yerqiang, Yulongkashi and Keliya (10.86-23.27% and 29.16-35.95%, respectively); less for the East Asian monsoon-dominated basins such as Yellow, Yangtze and Bayin (0-0.96% and 9.42-20.05%, respectively) (Table 2).

<Figure 1, here please, thanks>

<Table 2, here please, thanks>

带格式的: 字体颜色: 自动设置

**2.2 Methods**

**2.2.1 Water balance-based ET estimation**

The basin-wide water balance at the monthly and annual timescales could be written as the principle of mass conservation (also known as the continuity equation, Oliveira et al., 2014) of basin-wide precipitation (P, mm), evapotranspiration (ET<sub>wb</sub>, mm), runoff (Q, mm) as well as terrestrial water storage change (ΔS, mm),

$$ET_{wb} = P - Q - \Delta S \tag{1}$$

254 The terrestrial water storage ( $\Delta S$ ) in Eq. (1) includes the surface, subsurface and  
 255 ground water changes. It has been demonstrated that  $\Delta S$  cannot be neglected in water  
 256 balance calculation over monthly and annual timescales due to snow cover change  
 257 and anthropogenic interferences (e.g., reservoir operation, agricultural water  
 258 withdrawal) (Liu et al., 2016a). For the period 2002-2011, we calculated basin-wide  
 259 ET ( $ET_{wb}$ ) directly using the GRACE-derived  $\Delta S$  in Eq. (1). Since GRACE data is  
 260 absent before 2002, we calculated the monthly  $ET_{wb}$  using the following two-step  
 261 bias-correction procedure (Li X. et al., 2014). We defined  $P - Q$  in Eq. (1) as biased  
 262 ET ( $ET_{biased}$ , available from 1982 to 2011) relative to the “true” ET ( $ET_{wb} = P - Q -$   
 263  $\Delta S$ , available during the period 2002-2011 when the GRACE data is available). Over  
 264 the period 2002-2011, we first fitted  $ET_{biased}$  and  $ET_{wb}$  series separately using  
 265 different gamma distributions, which has been evidenced as an proper method for  
 266 modeling the probability distribution of ET (Bouraoui et al., 1999). The monthly  
 267  $ET_{biased}$  series (2002-2011) can then be bias-corrected through the inverse function  
 268 ( $F^{-1}$ ) of the gamma cumulative distribution function (CDF,  $F$ ) of  $ET_{wb}$  by matching  
 269 the cumulative probabilities between two CDFs as follow (Liu et al., 2016a),

$$270 \quad ET_{corrected}(m) = F^{-1}(F(ET_{biased}(m)|\alpha_{biased}, \beta_{biased})|\alpha_{wb}, \beta_{wb}) \quad (2)$$

271 Here  $\alpha_{biased}$ ,  $\beta_{biased}$  and  $\alpha_{wb}$ ,  $\beta_{wb}$  are shape and scale parameters of  
 272 gamma distributions for  $ET_{biased}$  and  $ET_{wb}$ .  $ET_{corrected}(m)$  and  $ET_{biased}(m)$   
 273 represent the monthly corrected and biased ET, respectively. The bias correction  
 274 procedure can be flexibly applied to the period 1983-2011 by matching the CDF  
 275 of  $ET_{biased}$  (1983-2011) to that of  $ET_{corrected}$  (2002-2011). The second step of  
 276 bias correction is to eliminate the annual bias through the ratio of annual  
 277  $ET_{biased}$  to annual  $ET_{corrected}$  calculated in the first step using the following  
 278 method,

$$ET_{\text{final}}(m) = \frac{ET_{\text{biased}}(a)}{ET_{\text{corrected}}(a)} \times ET_{\text{corrected}}(m) \quad (3)$$

where  $ET_{\text{final}}(m)$  is the final monthly ET after bias correction.  $ET_{\text{biased}}(a)$  and  $ET_{\text{corrected}}(a)$  represent the annual biased and corrected ET while  $ET_{\text{corrected}}(m)$  is the monthly corrected ET obtained from the first step. The procedure was then applied to correct the monthly  $ET_{\text{biased}}$  series and calculated the monthly  $ET_{\text{corrected}}$  during the period 1982-2001 for all TP basins. We take these results as sufficient representation of the “true” ET ( $ET_{\text{wb}}$ ) for evaluating multiple ET products and trend analysis.”

### 2.2.2 Modified Mann-Kendall test method

The Mann-Kendall (MK) test is a rank-based nonparametric approach which is less sensitive to outlier relative to other parametric statistics, but it is sometimes influenced by the serial correlation of time series. Pre-whitening is often used to eliminate the influence of lag-1 autocorrelation before the use of MK test. For example,  $X(X_1, X_2, \dots, X_n)$  is a time series data, it will be replaced by  $(X_2 - cX_1, X_3 - cX_2, \dots, X_{n+1} - cX_n)$  in pre-whitening if the lag-1 autocorrelation coefficient ( $c$ ) is larger than 0.1 (von Storch, 1995). However, significant lag-1 autocorrelation may still be detected after pre-whitening because only the lag-1 autocorrelation is considered in pre-whitening (Zhang et al., 2013). Moreover, it sometimes underestimate the trend for a given time series (Yue et al., 2002). Hamed and Rao (1998) proposed a modified version of MK test (MMK) to consider the lag- $i$  autocorrelation and related robustness of the autocorrelation through the use of equivalent sample size, which has been widely used in previous studies during the last five decades (McVicar et al., 2012; Zhang et al., 2013; Liu and Sun, 2016). In the MMK approach, if the lag- $i$  autocorrelation coefficients are significantly distinct from

zero, the original variance of MK statistics will be replaced by the modified one. In this study, we used the MMK approach to quantify the trends of water budget components in 18 TP basins and the significance of trend was tested at the >95% confidence level.

### 3 Results and Discussion

#### 3.1 ET evaluation and General hydrological characteristics of 18 TP basins

We first assessed the VIC\_IGSNRR simulated runoff against the observations for each basin (for example, at Tangnaihui and Pangduo stations in Fig.2). If the Nash Efficiency coefficient (NSE) between the observation and simulation is above 0.65, the VIC\_IGSNRR simulated runoff is acceptable and could be used to replace the missing runoff values for a given basin. Moreover, the CMA precipitation is consistent with TRMM (Corr = 0.86, RMSE = 8.34 mm/month) and IGSNRR forcing (Corr = 0.94, RMSE = 7.15mm/month) precipitation for multiple basins (i.e., for the smallest basin above Tongren station, Fig.2). Moreover, the magnitudes of GRACE-derived annual mean water storage change ( $\Delta S$ ) in 18 TP basins are relatively less than those for other water balance components such as annual P, Q and ET (Table 2 and Table 3). The uncertainties among GRACE-derived annual mean  $\Delta S$  from different data processing centers (CSR, GFZ and JPL) are small for 18 basins except for the basins controlled by Gadatan and Tangnaihui stations.

< Figure 2, here please, thanks>

< Table 3, here please, thanks>

We then evaluated six ET products in 18 TP basins against our calculated  $ET_{wb}$  at a monthly basis during the period 1983-2006 (Fig. 3). The ranges of monthly averaged ET among different basins (approximately 4–39 mm/month) are very close for all

带格式的: 字体颜色: 自动设置

products compare to that calculated from the  $ET_{wb}$  (6–42 mm/month). However, GLEAM\_E (correlation coefficient:  $Corr = 0.85$  and root-mean-square-error:  $RMSE = 5.69$  mm/month) and VIC\_E ( $Corr = 0.82$  and  $RMSE = 6.16$  mm/month) perform relatively better than others. Although Zhang\_E and GNoah\_E were found closely correlated to monthly  $ET_{wb}$  in the upper Yellow River, the upper Yangtze River, Qiangtang and Qaidam basins (Li X. et al., 2014), they did not exhibit overall good performances ( $Corr = 0.61$ ,  $RMSE = 7.97$  mm/month for Zhang\_E and  $Corr = 0.42$ ,  $RMSE = 10.16$  mm/month for GNoah\_E) for 18 TP basin used in this study. We thus use GLEAM\_E and VIC\_E together with  $ET_{wb}$  to analyze the seasonal cycles and trends of ET in 18 TP basins in the following sections.

< Figure 3, here please, thanks>

带格式的: 字体颜色: 自动设置

To investigate the general hydroclimatic characteristics of river basins over the TP, we classify 18 basins into three categories, namely westerlies-dominated basins (Yerqiang, Yulongkashi and Kelia), Indian monsoon-dominated basins (Brahmaputra and Salween), and East Asian monsoon-dominated basins (Yellow, Yalong and Yangtze) referred to Tian et al. (2007), Yao et al. (2012) and Dong et al. (2016). Interestingly, they are clustered into three groups under Budyko framework (Budyko, 1974; Zhang D. et al., 2016) with relatively lower evaporative index in Indian monsoon-dominant basins and higher aridity index in westerlies-dominant basins, which reveal various long-term hydroclimatologic conditions (Fig. 4). Overall, from the westerlies-dominant, Indian monsoon-dominant to East Asian monsoon-dominant basins, the annual mean air temperature ( $-5.68$ – $-0.97$  °C) and ET (and thus runoff coefficient gradually decreases) increases while the multiyear mean glacier area (and thus the glacier melt normalized by precipitation) gradually decreases (Fig. 4 and Table 2). Moreover, the vegetation status (NDVI range: 0.05–0.43; LAI range:

0.03-0.83) tends to be better. The  $R^2$  between basin-averaged NDVI and ET (0.76) is much higher than that between T and NDVI (0.35), which indicating that the water availability plays a more important role than the heat stress (i.e., colder status) over such basins. The results are in line with Shen et al. (2015), which indicated that the spatial pattern of ET trend was significantly and positively correlated with NDVI trend over the TP. The dominant climate systems are overall discrepant for the three TP regions with different water-energy characteristics and sources of water vapor. For example, in the westerlies-controlled basins, more glaciers developed due to their relatively colder air temperature and special seasonality of precipitation. Therefore, there are more snow melt contributions to total river streamflow with global warming during the period 1983-2006. It is a general picture of hydrological regime in high-altitude and cold regions (Zhang et al., 2013; Cuo et al., 2014), which could be interpreted from the perspective of multi-source datasets in the data-sparse TP.

< Figure 4, here please, thanks>

### 3.2 Seasonal cycles of basin-wide water budget components for the TP basins

The multi-year means of water budget components (i.e., P, Q, ET, snow cover and SWE) and vegetation parameters (i.e., NDVI and LAI) are calculated for each calendar month and for 18 TP river basins using multi-source datasets available from 1982 to 2011. Overall, the seasonal variations of P, Q, ET, air temperature and vegetation parameters are similar in all TP basins with peak values occurred in May to September (Fig.5 and Fig.6). The seasonal cycles of snow cover and SWE are generally consistent among the basins (the peak values mainly occur from October to next April, Fig.7). With the ascending air temperature from cold to warm months, the

带格式的: 字体颜色: 自动设置

379 basin-wide precipitation increases and vegetation cover expands gradually (the  
380 basin-wide ET also increase). Meanwhile, snow cover and glaciers retreat gradually  
381 with the melt water supplying the river discharge together with precipitation. The  
382 inter-basin variations of hydrological regime are to a large extent linked to the climate  
383 systems that prevail over the TP.

384 | < Figure 5, here please, thanks>

带格式的: 字体颜色: 自动设置

385 Although the temporal patterns of hydrological components are generally analogous,  
386 they vary among the parameters, climate zones and even basins (Zhou et al., 2005).  
387 For example, relative to air temperature, the seasonal pattern of runoff is similar to  
388 precipitation which reveals that runoff is mainly controlled by precipitation in most  
389 TP basins. It is in agreement with that summarized by Cuo et al. (2014). In the  
390 westerlies-dominated basins, the peak values of precipitation and runoff mainly  
391 concentrate in June-August, which contribute approximately 68-82% and 67-78% of  
392 annual totals, respectively. During this period, the runoff always exceeds precipitation  
393 which indicates large contributions of glacier/snow-melt water to streamflow. It is  
394 consistent with the existing findings in Tarim River (Yerqiang, Yulongkashi and  
395 Keliya rivers are the major tributaries of Tarim River), which indicated that the melt  
396 water accounted for about half of the annual total streamflow (Fu et al., 2008). The  
397 ET (vegetation cover) in three westerlies-dominated basins are relatively less (scarcer)  
398 than that in other TP basins while the percentages of glacier and seasonal snow cover  
399 are higher in these basins which contribute more melt water to river discharge (Fig.6  
400 and Fig.7). Overall, the SWE in Yerqiang, Yulongkashi and Keliya rivers are higher in  
401 winter than other seasons, but they vary with basins and products which reflect  
402 considerable uncertainties in SWE estimations.

403 | < Figure 6, here please, thanks>

带格式的: 字体颜色: 自动设置

404 In the Indian monsoon and East Asian monsoon dominated basins, the runoff  
405 concentrates during June-September (or June- October) with precipitation being the  
406 dominant contributor of annual total runoff. For example, the peak values of  
407 precipitation and runoff occur during June-September at Zhimenda station  
408 (contributing about 80% and 74% of the annual totals) while those occur during  
409 June-October at Tangnaihai station (contributing about 78% and 71% of the annual  
410 totals, respectively). The results are quite similar to the related studies in eastern and  
411 southern TP such as Liu (1999), Dong et al. (2007), Zhu et al. (2011), Zhang et al.  
412 (2013), Cuo et al. (2014). The vegetation cover (ET) in most basins is denser (higher)  
413 than that in the westerlies-dominant basins. Moreover, the seasonal snow mainly  
414 covers from mid-autumn to spring and correspondingly the SWE is relatively higher  
415 in these months in all basins except for Yellow River above Xining station, Salwee  
416 River above Jiayuqiao station and Brahmaputra River above Nuxia and Yangcun  
417 stations.

418 | < Figure 7, here please, thanks>

带格式的: 字体颜色: 自动设置

### 419 3.3 Trends of basin-wide water budget components for the TP basins

420 The Q, P and  $ET_{wb}$  ~~all-overall~~ ascended under regional warming during the past 30  
421 years in the westerlies-dominated basins (Fig.8), except for P in the Yerqiang River  
422 basin (Kulukelangan station), but only Q in Keliya River basin (Numaitilangan station)  
423 showed statistically significantly increase at the 0.05 level. -The aridity index  
424 (PET/P), which is an indicator for the degree of dryness, slightly declined (not  
425 significant) in all basins in northwestern TP. Although both P and PET increased in  
426 the Keliya River basin since the 1980s (Shi et al., 2003; Yao et al., 2014), the PET/P  
427 declined due to the higher rates of the increase of P than that of PET. The climate  
428 moistening (Shi et al., 2003) in the headwaters of these inland rivers would be



beneficial to the water resources and oasis agro-ecosystems in the middle and lower basins. The increase in streamflow was also found in most tributaries of the Tarim River (Sun et al., 2006; Fu et al., 2010; Mamat et al., 2010). Moreover, the westerlies, revealed by the Asian Zonal Circulation Index (60°-150° E), slightly enhanced (linear trend: 0.21, P-value: 0.26) over the period 1982-2011 (Fig.9). With the strengthening westerlies, more water vapor may be transported and fell as rain or snow in northwestern TP (e.g., the eastern Pamir region). Both SWE products (VIC\_IGSNRR simulated and GlobaSnow-2 product) showed marginally slightly increase across these basins with rising seasonal snow covers and glaciers (Yao et al., 2012). More precipitation was transformed into snow-/glacier and the runoff coefficient (Q/P) exhibited decrease with precipitation obviously increased (Fig.8). In addition, the transpiration in these basins might overall decrease with vegetation degradation (Yin et al., 2016) as revealed by— the NDVI and LAI (Yin et al., 2016)—(both decrease significantly in all westerlies-dominated basins except NDVI in Yerqiang and Yulongkashi rivers) but the atmospheric evaporative demand indicated by CRU PET increased (significantly increase in the Yulongkashi and Keliya rivers) during the period 1982-2011.

< Figure 8, here please, thanks>

< Figure 9, here please, thanks>

In the East Asian monsoon dominated basins, there are two types of change for basin-wide water budget components. For example, P and Q showed marginally decrease slightly decreased in the upper Yellow River (Tangnihai, Huangheyan and Jimai stations) and Yalong River (Yajiang station) but slightly increased in other basins (Zelingou, Gandatan, Xining, Tongren and Zhimenda stations) over the period of 1982-2011 (Fig.10). Only P in Zhimenda station exhibited statistically significant

带格式的: 字体颜色: 自动设置

increase at the 0.05 level. The declined Q and P in the upper Yellow and Yalong Rivers (located at the eastern Tibetan Plateau) were consistent with that found by Cuo et al. (2013, 2014) and Yang et al. (2014), and were in line with the weakening East Asian Summer Monsoon (linear slope: -0.01, P-value: 0.56) (Fig.9). The vegetation turned green markedly while  $ET_{wb}$  and PET increased (distinctly trends were found for  $ET_{wb}$  in basins controlled by Zelingou, Tangnaihai and Zhimenda and for PET in all rivers except for basins controlled by Xining, Tongren and Zhimenda stations) in all East Asian monsoon dominated basins (except for  $ET_{wb}$  in the basins above Tongren and Yajing stations) with the significantly ascending air temperature during the period 1982-2011. The aridity index (PET/P) slightly decreased in all basins (significantly decrease was found in the upper Yangtze River basin above Zhimenda station) except for the upper Yellow River basin above Jimai station and the upper Yalong River basin above Yajiang station. Moreover, the SWE, ~~however, both the runoff coefficients and SWE showed slight but insignificant decrease in most East Asian monsoon dominated basins (SWE VIC exhibited markedly decline in basins above Tangnaihai, Huangheyuan and Zhimenda stations while SWE Globsnow showed significantly decrease in basins above Xining station) decreased~~ except for the Bayin River above Zelingou station and the upper Yellow River above Tongren station in the East Asian monsoon dominated basins.

< Figure 10, here please, thanks >

The P,  $ET_{wb}$  and Q also increased slightly in the Indian monsoon-dominated basins (except for  $ET_{wb}$  in the basin above Yangcun station) such as Salween River and Brahmaputra River (Fig.11), which are in line with the strengthening (linear trend: 0.01, P-value: 0.12) of the Indian summer monsoon (revealed by the Indian Ocean Dipole Mode Index) during the specific period 1982-2011 (Fig.9). However, only P in

带格式的: 字体颜色: 自动设置

basins above Nuxia and Yangcun stations,  $Q$  in Nuxia station as well as  $ET_{wb}$  in  
basins above Jiayuqiao, Pangduo, Tangjia and Yangcun showed statistically  
significant trends at the 0.05 level. The slightly increasing trend of annual streamflow  
at Jiayuqiao station was ~~For example, at Jiayuqiao station, the annual streamflow~~  
~~showed a slightly increasing trend which was~~ consistent with that examined by Yao et  
al. (2012) during the period 1980-2000. The vegetation status, revealed by NDVI  
and LAI, turned better slightly (markedly trends were found in NDVI in basin above  
Gongbujiangda stations and LAI in all Indian monsoon-dominated basins except for  
one above Pangduo station) associated with the ascending air temperature. The aridity  
index (PET/P) exhibited slight but insignificant decrease ~~decreased~~ in all basins  
(markedly declined in basins above Nuxia and Yangcun stations) except for the  
Brahmaputra River above Tangjia station, which indicated that most basins in the  
Indian monsoon-dominated regions turned wetter over the period of 1982-2011. The  
increased PET/P in Brahmaputra River basin may be consistent with the drying  
moisture flux in the southeastern TP, as illustrated by Gao et al. (2014). ~~The~~  
runoff coefficient ( $Q/P$ ) slightly increased in basins above at Gongbujiangda and  
Nuxia stations while distinctly decreased in basins above at Jiayuqiao, ~~Pangduo,~~  
Tangji and Yangcun stations. Moreover, the basin-wide SWE Globsnow exhibited  
minor decrease ~~declined~~ in the upper Salween River and Brahmaputra River above  
~~Pangduo,~~ Tangjia and Gongbujiangda stations while significantly increased in  
Brahmaputra River above Nuxia and Yangcun stations.

< Figure 11, here please, thanks>

带格式的: 字体颜色: 自动设置

### 3.4 Uncertainties

The results may unavoidably associate with some uncertainties inherited from the  
multi-source datasets used. The primary sources of uncertainty may arise from the

precipitation inputs. We compared the seasonal cycles and annual trends in different precipitation products, i.e. CMA\_P, IGSNRR\_P and TRMM\_P (and their calculated  $ET_{wb}$  from the water balance) during the period 2000-2011 (Fig. 12 and Fig. 13). We found there are some uncertainties among different precipitation products and thus among their estimated  $ET_{wb}$ , especially in the westerlies-dominated basins. However, for each basin, the seasonal cycles of precipitation (and their calculated  $ET_{wb}$ ) calculated from different products are overall similar (especially for the observation-based products, CMA\_P and IGSNRR\_P). The signs of trend for annual CMA\_P and IGSNRR\_P (and their calculated  $ET_{wb}$ ) are consistent in most river basins (i.e., 14 out 18 basins for two precipitation products and 17 out 18 basins for their calculated  $ET_{wb}$ ) during the period 1982-2011. The consistency of trends between two precipitation products, to some extent, revealed that the trends in CMA\_P were not obviously influenced by the changing density of rain gauges in TP basins. Although some uncertainties exist due to limited and unevenly distributed meteorological stations used in the plateau and the influences of complex terrain, CMA\_P is still the best observation-based precipitation product nowadays in China which could be applied to hydrological studies in the TP.

< Figure 12, here please, thanks>

< Figure 13, here please, thanks>

带格式的: 字体颜色: 自动设置

Although the seasonal cycles of  $ET_{wb}$  could be captured by GLEAM\_E and VIC\_E, they still have considerable uncertainties at some stations (e.g., Numaitilangan, Gongbujiangda and Nuxia) (Fig.5). Compared to the annual trend of  $ET_{wb}$  (Table 4), most ET products (including the well-performed GLEAM\_E and VIC\_E) could not detect the decreasing trends in 7 out of 18 basins (Kulukelangan, Tongguziluoke, Xining, Tongren, Jimai, Nuxia and Gongbujiangda) due to their different forcing data,

algorithm used as well as varied spatial-temporal resolutions (Xue et al., 2013; Li et al., 2014; Liu et al., 2016a). In particular, it is well known that land surface models have some difficulties (e.g., parameter tuning in boundary layer schemes) when applying to the TP, even though they sometimes have good performances in different regions/basins (Xia et al., 2012; Bai et al., 2016). For example, Xue et al. (2013) indicated that GNoah\_E underestimated the  $ET_{wb}$  in the upper Yellow River and Yangtze River basins on the Tibetan Plateau mainly due to its negative-biased precipitation forcing. We thus only used  $ET_{wb}$  in the trend detection of water budget components in Fig.8, Fig.10 and Fig.11 in this study. The two SWE products also showed large uncertainty with respect to both their seasonal cycles and trends. The VIC\_IGSNRR simulated and GlobaSnow-2 SWEs have not been validated in the TP due to the lack of snow water equivalent observations, but in some basins (e.g., Zelingou and Numaitilangan) they showed similar seasonal cycles and annual trends.

<Table 4, here please, thanks>

The interpolation of missing values of runoff with VIC\_IGSNRR simulated runoff and the gridded precipitation data (which interpolated from limited gauged precipitation over the plateau) also introduced uncertainties. There are also considerable uncertainties arising from empirical extending the ET series back prior to the GRACE era. However, the trends in  $ET_{wb}$  have not significantly affected by erroneous trends in the precipitation inputs to the bias-correction based water balance calculation. For example, the trends in CMA\_P and IGSNRR\_P are opposite in few basins (No. 01, 07, 08, 13 in Fig. 13), but the trends in their calculated  $ET_{wb}$  are both consistent for each basin. It is, to some extent, certified the effectiveness of the bias correction-based ET-estimate approach. With these caveats, we can interpret the general hydrological regimes and their responses to the changing climate in the TP

带格式的: 字体颜色: 自动设置

basins from solely the perspective of multi-source datasets, which are comparable to the existing studies based on the in situ observations and complex hydrological modeling.

#### **4 Summary**

In this study, we investigated the seasonal cycles and trends of water budget components in 18 TP basins during the period 1982-2011, which is not well understood so far due to the lack of adequate observations in the harsh environment, through integrating the multi-source global/regional datasets such as gauge data, satellite remote sensing and land surface model simulations. By using a two-step bias correction procedure, we calculated the annual basin-wide  $ET_{wb}$  through the water balance approach considering the impacts of water storage change. We found that the GLEAM\_E and VIC\_E perform better relative to other products against the calculated  $ET_{wb}$ .

From the Budyko framework perspective, the general water and energy budgets are different in the westerlies-dominated (with higher aridity index, runoff coefficient and glacier cover), the Indian monsoon-dominated and the East Asian monsoon-dominated (with higher air temperature, vegetation cover and evapotranspiration) basins. In the 18 TP basins, precipitation is the major contributor to the river runoff, which concentrates mainly during June-October (June-August for the westerlies-dominated basins, June-September or June to October for the Indian monsoon-dominated and the East Asian monsoon-dominated basins). The basin-wide SWE is relatively high from mid-autumn to spring for all 18 TP basins except for Keliya River and Brahmaputra River above the Nuxia and Yangcun stations. The

vegetation cover is relatively less whereas snow/glacier cover is more in the westerlies-dominant basins compared to other basins.

During the period 1982-2011, ~~we found that~~ the P, Q and  $ET_{wb}$  showed slight but insignificant increase~~increased~~ across most of the basins in Tibetan Plateau with the exception of some tributaries located at the upper Yellow River and Yalong River due to the weakening East Asian monsoon. The aridity index (PET/P) exhibited an indistinctively decrease-decreasing trend in most TP basins which corresponds to the warming and moistening climate in the TP and western China. Moreover, the runoff coefficient (Q/P) declined marginally in most basins which may be, to some extent, due to ET increase induced by vegetation greening and the influences of snow and glacier changes. Although there are considerable uncertainties inherited from multi-source data used, the general hydrological regimes in the TP basins could be revealed, which are consistent to the existing results obtained from in situ observations and complex land surface modeling. It indicates the usefulness of integrating the multiple datasets (e.g., in situ observations, remote sensing-based products, reanalysis outputs, land surface model simulations and climate model outputs) for hydrological applications. The generalization here could be helpful for understanding the hydrological cycle and supporting sustainable water resources management and eco-environment protection in the Tibetan Plateau.

**Author contributions.** Wenbin Liu and Fubao Sun developed the idea to see the general water budgets in the TP basins from the perspective of multisource datasets. Wenbin Liu collected and processed the multiple datasets with the help of Yanzhong Li, Guoqing Zhang, Wee Ho Lim, Hong Wang as well as Peng Bai, and prepared the

manuscript. The results were extensively commented and discussed by Fubao Sun,  
Jiahong Liu and Yan-Fang Sang.

**Acknowledgements.** This study was supported by the National Key Research and  
Development Program of China (2016YFC0401401 and 2016YFA0602402), National  
Natural Science Foundation of China (41401037, [41601035](#), [91647110](#), [41701019](#)  
and 41330529), the Open Research Fund of State Key Laboratory of Desert and Oasis  
Ecology in Xinjiang Institute of Ecology and Geography, Chinese Academy of  
Sciences (CAS), [the Key Research Program of the CAS \(ZDRW-ZS-2017-3-1\)](#), the  
CAS Pioneer Hundred Talents Program (Fubao Sun), the CAS President's  
International Fellowship Initiative (2017PC0068) and the program for the "Bingwei"  
Excellent Talents from the Institute of Geographic Sciences and Natural Resources  
Research, CAS. We are grateful to the NASA MEaSUREs Program (Sean Swenson)  
for providing the GRACE land data processing algorithm. The basin-wide water  
budget series in the TP Rivers used in this study are available from the authors upon  
request ([liuwb@igsnr.ac.cn](mailto:liuwb@igsnr.ac.cn)). We thank [Axel Kleidon](#), the editors and reviewers for  
their invaluable comments and constructive suggestions.

## References

- Akhtar, M., Ahmad, N., and Booij, M.J.: Use of regional climate model simulations as input for  
hydrological models for the Hindukush-Karakorum-Himalaya region, Hydrol. Earth Syst. Sci.  
13, 1075-1089, 2009.
- Bai, P., Liu, X.M., Yang, T.T., Liang, K., and Liu, C.M.: Evaluation of streamflow simulation  
results of land surface models in GLDAS on the Tibetan Plateau, J. Geophys. Res. Atmos., 121,  
12180-12197, 2016.
- Berrisford, P, Lee, D., Poli, P., Brugge, R., Fielding, K., Fuentes, M., Kallberg, P., Kobayashi, S.,



630 Uppala, S., and Simmons, A.: The ERA-interim archive. ERA Reports Series No. 1 Version 2.0,  
 631 Available from: <[https://www.researchgate.net/publication/41571692\\_The\\_ERA-interim](https://www.researchgate.net/publication/41571692_The_ERA-interim_archive)  
 632 archive>, 2011.

633 Bookhagen, B. and Burbank, D.W.: Toward a complete Himalayan hydrological budget:  
 634 spatiotemporal distribution of snowmelt and rainfall and their impact on river discharge, J.  
 635 Geophys. Res., 115, F03019, 2010.

636 Bouraoui, F., Vachaud, G., Li, L.Z.X., LeTreut, H., and Chen, T.: Evaluation of the impact of  
 637 climate changes on water storage and groundwater recharge at the watershed scale, Clim. Dyn.,  
 638 15(2), 153-161, 1999.

639 Budyko, M.I.: Climate and life. Academic Press, 1974.

640 Chen, D., Xu, B., Yao, T., Guo, Z., Cui, P., Chen, F., Zhang, R., Zhang, X., Zhang, Y., Fan, J., Hou,  
 641 Z., and Zhang, T.: Assessment of past, present and future environmental changes on the Tibetan  
 642 Plateau, Chinese SCI. Bull., 60(32), 3025-3035, 2015 (in Chinese).

643 Cuo, L., Zhang, Y.X., Bohn, T.J., Zhao, L., Li, J.L., Liu, Q.M., and Zhou, B.R.: Frozen soil  
 644 degradation and its effects on surface hydrology in the northern Tibetan Plateau, J. Geophys.  
 645 Res. Atmos., 120(6), 8276-8298, 2015.

646 Cuo, L., Zhang, Y.X., Gao, Y., Hao, Z., and Cairang, L.: The impacts of climate change and land  
 647 cover/use transition on the hydrology in the upper Yellow River Basin, China, J. Hydrol., 502,  
 648 37-52, 2013.

649 Cuo, L., Zhang, Y.X., Zhu, F.X., and Liang, L.Q.: Characteristics and changes of streamflow on  
 650 the Tibetan Plateau: A review, J. Hydrol. Reg. stud., 2, 49-68, 2014.

651 Dong, X., Yao, Z., and Chen, C.: Runoff variation and responses to precipitation in the source  
 652 regions of the Yellow River, Resour. Sci., 29(3), 67-73, 2007 (in Chinese).

653 Dong, W., Lin, Y., Wright, J.S., Ming, Y., Xie, Y., Wang, B., Luo, Y., Huang, W., Huang, J., Wang,  
 654 L., Tian, L., Peng, Y., and Xu, F.: Summer rainfall over the southwestern Tibetan Plateau  
 655 controlled by deep convection over the Indian Subcontinent, Nat. Commun., 7, 10925, 2016.

656 Duan, A.M. and Wu, G.X.: Change of cloud amount and the climate warming on the Tibetan  
 657 Plateau, Geophys. Res. Lett., 33, L22704, 2006.

658 Fu, L., Chen, Y., Li, W., Xu, C., and He, B.: Influence of climate change on runoff and water  
 659 resources in the headwaters of the Tarim River, Arid Land Geogr., 31(2), 237-242, 2008 (in  
 27 / 61

Chinese).

Fu, L., Chen, Y., Li, W., He, B., and Xu, C.: Relation between climate change and runoff volume in the headwaters of the Tarim River during the last 50 years., *J. Desert Res.*, 30(1), 204-209, 2010 (in Chinese).

Gao, Y.H., Cuo, L., and Zhang, Y.X.: Changes in moisture flux over the Tibetan Plateau during 1979-2011 and possible mechanisms, *J. Climate*, 27, 1876-1893, 2014.

Guo, W.Q., Liu, S.Y., Yao, X.J., Xu, J.L., Shangguan, D.H., Wu, L.Z., Zhao, J.D., Liu, Q., Jiang, Z.L., Wei, J.F., Bao, E.J., Yu, P.C., Ding, L.F., Li, G., Ge, C.M., and Wang, Y.: The Second Glacier Inventory Dataset of China, Cold and Arid Regions Science Data Center at Lanzhou, doi: 10.3972/glacier.001.2013.db, 2014.

Hamed, K.H. and Rao, A.R.: A modified Mann-Kendall trend test for autocorrelation data, *J. Hydrol.*, 204(1-4), 182-196, 1998.

Huffman, G.J., , E.F., Bolvin, D.T., Nelkin, E.J., and Adler, R.F.: last updated 2013: TRMM Version 7 3B42 and 3B43 Data Sets, NASA/GSFC, Greenbelt, MD. Data set accessed at <http://mirador.gsfc.nasa.gov/cgi-bin/mirador/presentNavigation.pl?tree=project&project=TRMM&dataGroup=Gridded&CGIS=ESSID=5d12e2ffa38ca2aac6262202a79d882a>, 2012.

Harris, I., Jones, P.D., Osborn, T.J., and Lister, D.H.: Updated high-resolution grids of monthly climatic observations – the CRU TS3.10 Dataset, *Int. J. Climatol.*, 34 (3), 623-642, 2014.

Immerzeel, W.W., van Beek, L.P.H., and Bierkens, M.F.P.: Climate change will affect the Asian water towers, *Science*, 328, 1382-1385, 2010.

Jung, M., Reichstein, M., Ciais, P., Seneviratne, S.I., Sheffield, J., Goulden, M.L., Bonan, G., Cescatti, A., Chen, J., de Jeu, R., Dolman, A.J., Eugster, W., Gerten, D., Gianelle, D., Gobron, N., Heinke, J., Kimball, J., Law, B.E., Montagnani, L., Mu, Q., Mueller, B., Oleson, K., Papale, D., Richardson, A.D., Rouspard, O., Running, S., Tomelleri, E., Viovy, N., Weber, U., Williams, C., Wood, E., Zaehle, S., and Zhang, K.: Recent decline in the global land evapotranspiration trend due to limited moisture supply, *Nature*, 467, 951-954, 2010.

Kobayashi, S., Ota, Y., Harada, Y., Ebita, A., Moriya, M., Onoda, H., Onogi, K., kamahori, H.,

kobayashi, C., Endo, H., miyaoka, K., and Takahashi, K.: The JRA-55 Reanalysis: General specifications and basic characteristics, *J.Meteor. Soc. Japan*, 93(1), 5-58, doi: 10.2151/jmsj.2015-001, 2015.

Landerer, F.W. and Swenson, S.C.: Accuracy of scaled GRACE terrestrial water storage estimates, *Water Resour.Res.*, 48, W04531, 2012.

Li, F.P., Zhang, Y.Q., Xu, Z.X., Liu, C.M., Zhou, Y.C., and Liu, W.F.: Runoff predictions in ungauged catchments in southeast Tibetan Plateau, *J. Hydrol.*, 511, 28-38, 2014.

Li, F.P., Zhang, Y.Q., Xu, Z.X., Teng, J., Liu, C.M., Liu, W.F., and Mpelasoka, F.: The impact of climate change on runoff in the southeastern Tibetan Plateau, *J. Hydrol.*, 505, 188-201, 2013.

Li, J.P. and Zeng, Q.C.: A unified monsoon index, *Geophy. Res. Lett.*, 29(8), 1274, 2002.

Li, X.P., Wang, L., Chen, D.L., Yang, K., and Wang, A.H.: Seasonal evapotranspiration changes (1983-2006) of four large basins on the Tibetan Plateau, *J. Geophys. Res.*, 119 (23), 13079-13095, 2014.

Liang, S.L. and Xiao, Z.Q.: Global Land Surface Products: Leaf Area Index Product Data Collection(1985-2010), Beijing Normal University, doi:10.6050/glass863.3004.db, 2012.

Liu, T.: Hydrological characteristics of Yalungzangbo River, *Acta Geogr. Sin.*, 54 (Suppl.), 157-164, 1999 (in Chinese).

Liu, W.B. and Sun, F.B.: Assessing estimates of evaporative demand in climate models using observed pan evaporation over China, *J. Geophys. Res. Atmos.*, 121, 8329-8349, 2016.

Liu, W.B., Wang, L., Zhou, J., Li, Y.Z., Sun, F.B., Fu, G.B., Li, X.P., and Sang, Y-F.: A worldwide evaluation of basin-scale evapotranspiration estimates against the water balance method, *J. Hydrol.*, 538, 82-95, 2016a.

Liu, W.B., Wang, L., Chen, D.L., Tu, K., Ruan, C.Q., and Hu, Z.Y.: Large-scale circulation classification and its links to observed precipitation in the eastern and central Tibetan Plateau, *Clim. Dyn.*, 46, 3481-3497, 2016b.

Liu, X.M., Yang, T., Hsu, K., Liu, C., and Sorooshian, S.: Evaluating the streamflow simulation capability of PERSIANN-CDR daily rainfall products in two river basins on the Tibetan Plateau, *Hydrol. Earth Syst. Sci.*, 21, 169-181, 2017.

Long, D., shen, Y.J., Sun, A., Hong, Y., Longuevergne, L., Yang, Y.T., Li, B., and Chen, L.:  
Drought and flood monitoring for a large karst plateau in Southwest China using extended  
GRACE data, *Remote Sen. Environ.*, 155, 145-160, 2014.

Lucchesi, R.: File specification for MERRA products, GMAO Office Note No.1 (version 2.3), 82  
pp, available from [http://gmao.gsfc.nasa.gov/pubs/office\\_notes](http://gmao.gsfc.nasa.gov/pubs/office_notes), 2012.

Ma, N., Szilagyi, J., Niu, G.Y., Zhang, Y.S., Zhang, T., Wang, B.B., and Wu, Y.H.: Evaporation  
variability of Nam Co Lake in the Tibetan Plateau and its role in recent rapid lake expansion, *J.*  
*Hydrol.*, 537, 27-35, 2016.

Ma, N., Zhang, Y.S., Guo, Y.H., Gao, H.F., Zhang, H.B., and Wang, Y.F.: Environmental and  
biophysical controls on the evapotranspiration over the highest alpine steppe, *J. Hydrol.*, 529,  
980-992, 2015.

Mamat, A., Halik, W., and Yang, X.: The climatic changes of Qarqan river basin and its impact on  
the runoff, *Xinjiang Agric. Sci.*, 47 (5), 996-1001, 2010 (in Chinese).

McVicar, T.R., Roderick, M., Donohue, R.J., Li, L.T., Van Niel, T.G., Thomas, A., Grieser, J.,  
Jhajharia, D., Himri, Y., Mahowald, N.M., Mescherskaya, A.V., Kruger, A.C., Rehman, S., and  
Dinpashoh, Y.: Global review and synthesis of trends in observed terrestrial near-surface wind  
speeds: implications for evaporation, *J. Hydrol.*, 416-417, 182-205, 2012.

Miralles, D.G., De Jeu, R.A.M., Gash, J.H., Holmes, T.R.H., and Dolman, A.J.: Magnitude and  
variability of land evaporation and its components at the global scale, *Hydrol. Earth Syst. Sci.*, 15,  
967-981, 2011.

Miralles, D.G., Gash, J.H., Holmes, T.R.H., de Jeu, R.A.M, and Dolman, A.J.: Global canopy  
interception from satellite observations, *J. Geophys. Res.*, 115, D16122, 2010.

Oliveira, P.T.S., Mearing, M.A., Moran, M.S., Goodrich, D.C., Wendland, E., and Gupta, H.V.:  
Trends in water balance components across the Brazilian Cerrado, *Water Resour. Res.*, 50,  
7100-7114, 2014.

Rodell, M., Houser, P.R., Jambor, U., Gottschalck, J., Mitchell, K., Meng, C.-J., Arsenault, K.,  
Cosgrove, B., Radakovich, J., Bosilovich, M., Entin, J.K., Walker, P., Lohmann, D., and Toll, D.:  
The global land data assimilation system, *B. Am. Meteorol. Soc.*, 85, 381-394, 2004.

Rui, H.: README Document for Global Land Data Assimilation System Version 2 (GLDAS-2)  
Products, GES DISC, 2011.

746 Saji, N.H., Goswami, B.N., Vinayachandran, P.N., and Yamagata, T.: A dipole mode in the tropical  
747 Indian Ocean, *Nature*, 401, 360-363, 1999.

748 Shen, M.G., Piao, S.L., Jeong, S., Zhou, L.M., Zeng, Z.Z., Ciais, P., Chen, D.L., Huang, M.T., Jin,  
749 C.S., Li, L.Z.X., Li, Y., Myneni, R.B., Yang, K., Zhang, G.X., Zhang, Y.J., and Yao, T.D.:  
750 Evaporative cooling over the Tibetan Plateau induced by vegetation growth, *Proc. Natl. Acad.*  
751 *Sci. U. S.A.*, 112(30), 9299-9304, 2015.

752 Shi, Y.F., Shen, Y.P., Li, D.L., Zhang, G.W., Ding, Y.J., Hu, R.J., and Kang, E.S.: Discussion on  
753 the present climate change from Warm2dry to Warm2wet in northwest China, *Quat. Sci.*, 23(2),  
754 152-164, 2003 (in Chinese).

755 Shepard, D.S.: Computer mapping: the SYMAP interpolation algorithm. *Spatial Statistics and*  
756 *Models*, G.L. Gaile and C.J. Willmott, Eds., D. Reidel, 133-145, 1984.

757 Sun, B., Mao, W., Feng, Y., Chang, T., Zhang, L., and Zhao, L.: Study on the change of air  
758 temperature, precipitation and runoff volume in the Yarkant River basin, *Arid Zone Res.*, 23(2),  
759 203-209, 2006 (in Chinese).

760 Takala, M., Luoju, K., Pulliainen, J., Derksen, C., Lemmetyinen, J., Kärnä J.-P., Koskinen, J., and  
761 Bojkov, B.: Estimating northern hemisphere snow water equivalent for climate research through  
762 assimilation of spaceborne radiometer data and ground-based measurements, *Remote*  
763 *Sens. Environ.*, 115 (12), 3517-3529, 2011.

764 Tapley, B.D., Bettadpur, S., Watkins, M., and Reigber, C.: The gravity recovery and climate  
765 experiment: mission overview and early results, *Geophys. Res. Lett.*, 31, L09607, 2004.

766 Tian, L., Yao, T., MacClune, K., White, J.W.C., Schilla, A., Vaughn, B., Vachon, R., and  
767 Ichiyangi, K.: Stable isotopic variations in west China: a consideration of moisture sources, *J.*  
768 *Geophys. Res. Atmos.*, 112, D10112, 2007.

769 Tucker, C.J., Pinzon, J.E., Brown, M.E., Slayback, D., Pak, E.W., Mahoney, R., Vermote, E., and  
770 El Saleous, N.: An extended AVHRR 8 km NDVI data set compatible with MODIS and SPOT  
771 vegetation NDVI data, *Int. J. Remote Sens.*, 26(20), 4485-4498, 2005.

772 von Storch, H.: Misuses of statistical analysis in climate research, In *Analysis of Climate*  
773 *Variability: Applications of Statistical Techniques*, Springer-Verlag: Berlin, 11-26, 1995.

Wang, A. and Zeng, X.: Evaluation of multireanalysis products within site observations over the Tibetan Plateau, *J. Geophys. Res.*, 117, D05102, 2012.

Wang, L., Sun, L.T., Shrestha, M., Li, X.P., Liu, W.B., Zhou, J., Yang, K., Lu, H., and Chen, D.L.: Improving snow process modeling with satellite-based estimation of near-surface-air-temperature lapse rate, *J. Geophys. Res. Atmos.*, 121, 12005-12030, 2016.

Xia, Y., Mitchell, K., Ek, M., Cosgrove, B., Sheffield, J., Luo, L., Alonge, C., Wei, H., Meng, J., Livneh, B., and Duang, Q.: Continental-scale water and energy flux analysis and validation for North American Land Data Assimilation System project phase 2 (NLDAS-2): 2. Validation of model-simulated streamflow, *J. Geophys. Res. Atmos.*, 117(D3), D03110, 2012.

Xu, L.: The land surface water and energy budgets over the Tibetan Plateau, Available from Nature Precedings < <http://hdl.handle.net/10101/npre.2011.5587.1>>, 2011.

Xue, B.L., Wang, L., Yang, K., Tian, L., Qin, J., Chen, Y., Zhao, L., Ma, Y., Koike, T., Hu, Z., and Li, X.P.: Modeling the land surface water and energy cycle of a mesoscale watershed in the central Tibetan Plateau with a distributed hydrological model, *J. Geophys. Res. Atmos.*, 118, 8857-8868, 2013.

Yao, Z., Duan, R., and Liu, Z.: Changes in precipitation and air temperature and its impacts on runoff in the Nujang River basins. *Resour. Sci.* 34(2), 202-210, 2012 (in Chinese)

Yang, K., Qin, J., Zhao, L., Chen, Y.Y., Tang, W.J., Han, M.L., Lazhu, Chen, Z.Q., Lv, N., Ding, B.H., Wu, H., and Lin, C.G.: A multi-scale soil moisture and freeze-thaw monitoring network on the third pole, *Bull. Am. Meteorol. Soc.*, 94, 1907-1916, 2013.

Yang, K., Wu, H., Qin, J., Lin, C.G., Tang, W.J., and Chen, Y.Y.: Recent climate changes over the Tibetan Plateau and their impacts on energy and water cycle: a review, *Glob. Planet Change*, 112, 79-91, 2014.

Yao, T.D., Thompson, L., Yang, W., Yu, W.S., Gao, Y., Guo, X.J., Yang, X.X., Duan, K.Q., Zhao, H.B., Xu, B.Q., Pu, J.C., Lu, A.X., Xiang, Y., Kattel, D.B., and Joswiak, D.: Different glacier status with atmospheric circulations in Tibetan Plateau and surroundings, *Nat. Clim. Change*, 2, 1-5, 2012.

Yao, Y.J., Zhao, S.H., Zhang, Y.H., Jia, K., and Liu, M.: Spatial and decadal variations in potential evapotranspiration of China based on reanalysis datasets during 1982-2010, *Atmosphere*, 5, 737-754, 2014.

Yin, G., Hu, Z.Y., Chen, X., and Tiyyip, T.: Vegetation dynamics and its response to climate change in Central Asia, *J. Arid Land*, 8, 375, 2016.

Yu, J., Zhang, G., Yao, T., Xie, H., Zhang, H., Ke, C., and Yao, R.: Developing daily cloud-free snow composite products from MODIS Terra-Aqua and IMS for the Tibetan Plateau, *IEEE Trans. Geosci. Remote Sens.*, 54(4), 2171-2180, 2015.

Yue, S., Pilon, P., Phinney, B., Cavadias, G.: The influence of autocorrelation on the ability to detect trend in hydrological series, *Hydrol. Process.*, 16(9), 1807-1829, 2002.

Zhang, D., Liu, X., Zhang, Q., Liang, K., and Liu, C.: Investigation of factors affecting inter-annual variability of evapotranspiration and streamflow under different climate conditions. *J. Hydrol.*, 543, 759-769, 2016.

Zhang, G., Xie, H., Yao, T., Liang, T., and Kang, S.: Snow cover dynamics of four lake basins over Tibetan Plateau using time series MODIS data (2001-2100), *Water Resour. Res.*, 48(10), W10529, 2012.

Zhang, K., Kimball, J.S., Nemani, R.R., and Running, S.W.: A continuous satellite-derived global record of land surface evapotranspiration from 1983 to 2006, *Water Resour. Res.*, 46(9), W09522, 2010.

Zhang, L., Su, F., Yang, D., Hao, Z., and Tong, K.: Discharge regime and simulation for the upstream of major rivers over Tibetan Plateau, *J. Geophys. Res. Atmos.*, 118(15), 8500-8518, 2013.

Zhang, Q., Li, J., Singh, V., and Xu, C.: Copula-based spatial-temporal patterns of precipitation extremes in China, *Int. J. Climatol.*, 33, 1140-1152, 2013.

Zhang, X., Tang, Q., Pan, M., and Tang, Y.: A long-term land surface hydrologic fluxes and states dataset for China, *J. Hydrometeorol.*, 15, 2067-2084, 2014.

Zhang, Y., Peña-Arancibia, J.L., McVicar, T.R., Chiew, F.H.S., Vaze, J., Liu, C.M., Lu, X.J., Zheng, H.X., Wang, Y.P., Liu, Y.Y., Miralles, D.G., and Pan, M.: Multi-decadal trends in global terrestrial evapotranspiration and its components, *Scientific Reports*, 6, 19124, 2016.

Zhang, Y., Liu, C., Tang, Y., and Yang, Y.: Trend in pan evaporation and reference and actual evapotranspiration across the Tibetan Plateau, *J. Geophys. Res.*, 112, D12110, 2007.

Zhou, C., Jia, S., Yan, H., and Yang, G.: Changing trend of water resources in Qinghai Province from 1956 to 2000, *J. Glaciol. Geocryol.*, 27(3), 432-437, 2005 (in Chinese).

834 Zhou, J., Wang, L., Zhang, Y.S., Guo, Y.H., Li, X.P., and Liu, W.B.: Exploring the water storage  
835 changes in the largest lake (Selin Co) over the Tibetan Plateau during 2003-2012 from a  
836 basin-wide hydrological modeling,. *Water Resour. Res.*, 51, 8060-8086, 2015.

837 Zhou, S.Q., Kang, S., Chen, F., and Joswiak, D.R.: Water balance observations reveal significant  
838 subsurface water seepage from Lake Nam Co., south-central Tibetan Plateau,. *J. Hydrol.*, 491,  
839 89-99, 2013.

840 Zhu, Y., Chen, J., Chen, G.: Runoff variation and its impacting factors in the headwaters of the  
841 Yangtze River in recent 32 years, *J. Yangtze River Sci. Res. Inst.*, 28(6), 1-4, 2011 (in Chinese ).



842 | **Table 1:** Overview of multi-source datasets applied in this study

| Data category                   | Data source                                   | Spatial resolution | Temporal resolution | Available period used | Reference              |
|---------------------------------|---|--------------------|---------------------|-----------------------|------------------------|
| Runoff (Q)                      | Observed, National Hydrology Almanac of China | —                  | Daily               | 1982-2011             | —                      |
|                                 | VIC_IGSNRR simulated                          | 0.25°              | Daily               | 1982-2011             | Zhang et al. (2014)    |
| Precipitation (P)               | Observed, CMA                                 | 0.5°               | Monthly             | 1982-2011             | —                      |
|                                 | TRMM 3B43 V7                                  | 0.25°              | Monthly             | 2000-2011             | Huffman et al. (2012)  |
|                                 | IGSNRR forcing                                | 0.25°              | Daily               | 1982-2011             | Zhang et al. (2014)    |
| Temperature (Temp.)             | Observed, CMA                                 | 0.5°               | Monthly             | 2000-2011             | —                      |
| Terrestrial storage change (ΔS) | GRACE-CSR                                     | Approx.300-400 km  | Monthly             | 2002-2011             | Tapley et al. (2004)   |
|                                 | GRACE-GFZ                                     | Approx.300-400 km  | Monthly             | 2002-2011             | Tapley et al. (2004)   |
|                                 | GRACE-JPL                                     | Approx.300-400 km  | Monthly             | 2002-2011             | Tapley et al. (2004)   |
| Potential evaporation (PET)     | CRU   | 0.5°               | Monthly             | 1982-2011             | Harris et al. (2013)   |
| Actual evaporation (ET)         | MTE_E   | 0.5°               | Monthly             | 1982-2011             | Jung et al. (2010)     |
|                                 | VIC_E   | 0.25°              | Daily               | 1982-2011             | Zhang et al. (2014)    |
|                                 | GLEAM_E                                       | 0.25°              | Daily               | 1982-2011             | Miralles et al. (2011) |
|                                 | PML_E   | 0.5°               | Monthly             | 1982-2011             | Zhang Y et al. (2016)  |
|                                 | Zhang_E                                       | 8 km               | Monthly             | 1983-2006             | Zhang et al. (2010)    |
|                                 | GNoah_E                                       | 1.0°               | 3 hourly            | 1982-2011             | Rui (2011)             |
| NDVI                            | GIMMS NDVI dataset                            | 8 km               | 15 daily            | 1982-2011             | Tucker et al. (2005)   |
| LAI                             | GLASS LAI Product                             | 0.05°              | 8 daily             | 1982-2011             | Liang and Xiao (2012)  |
| Snow Cover                      | TP Snow composite Products                    | 500 m              | Daily               | 2005-2013             | Zhang et al. (2012)    |
| SWE                             | VIC_IGSNRR simulated                          | 0.25°              | Daily               | 1982-2011             | Zhang et al. (2014)    |
|                                 | GlobSnow-2 Product                            | 25 km              | Daily               | 1982-2011             | Takala et al. (2011)   |
| Glacier Area                    | the Second Glacier Inventory Dataset of China | —                  | —                   | 2005                  | Guo et al. (2014)      |

带格式的: 字体颜色: 自动设置

843 **Table 2:** Main features of the 18 TP river basins used in this study. The precipitation and temperature statistics for each basin were calculated from the observed  
844 CMA datasets while the NDVI and LAI statistics were extracted from the GIMMS NDVI dataset and GLASS LAI product. The GA% and SC% represented the  
845 percentages of multiyear-mean glacier cover and snow cover in each basin which were calculated from the Second Glacier Inventory Dataset of China and the daily  
846 TP snow cover dataset (2005-2013)  
847  
848

带格式的: 字体颜色: 自动设置

| No.  | Station       | Altitude<br>(m) | River name  | Drainage area<br>(km <sup>2</sup> ) | Multiyear-mean (1982-2011) and basin-averaged parameters |               |              |      |      |       |       |
|--|---------------|-----------------|-------------|-------------------------------------|--|---------------|--------------|------|------|-------|-------|
|  |               |                 |             |                                     | Q (mm/yr)  | Prec. (mm/yr) | Temp.(°C/yr) | NDVI | LAI  | GA%   | SC%   |
| <i><b>Westerlies-dominated basins:</b></i>         |               |                 |             |                                     |  |               |              |      |      |       |       |
| 01   | Kulukelangan  | 2000            | Yerqiang    | 32880.00                            | 158.60   | 128.34        | -5.68        | 0.05 | 0.03 | 10.97 | 35.03 |
| 02   | Tongguziluoke | 1650            | Yulongkashi | 14575.00                            | 151.56   | 134.04        | -4.07        | 0.06 | 0.04 | 23.27 | 35.95 |
| 03   | Numaitilangan | 1880            | Keliya      | 7358.00                             | 103.18   | 137.14        | -4.78        | 0.06 | 0.03 | 10.86 | 29.16 |
| <i><b>East Asian monsoon-dominated basins:</b></i> |               |                 |             |                                     |  |               |              |      |      |       |       |
| 04   |               | 4282            | Bayin       | 5544.00                             | 41.42  | 340.68        | -4.98        | 0.13 |      |       |       |
| 05   | Zelingou      | 3823            | Yellow      | 7893.00                             | 200.95   | 566.01        | -4.60        | 0.34 | 0.09 | 0.09  | 21.22 |
| 06   | Gadatan       | 3225            | Yellow      | 9022.00                             | 99.90  | 503.74        | 0.97         | 0.36 | 0.54 | 0.13  | 14.94 |
| 07   | Xining        | 3697            | Yellow      | 2832.00                             | 149.36   | 533.25        | -1.37        | 0.39 | 0.70 | 0.00  | 10.06 |
| 08   | Tongren       | 2632            | Yellow      | 121972.00                           | 159.48   | 540.32        | -2.40        | 0.34 | 0.83 | 0.00  | 9.42  |
| 09   | Tainaihai     | 4491            | Yellow      | 20930.00                            | 31.18  | 386.42        | -4.81        | 0.23 | 0.72 | 0.09  | 15.89 |
| 10   | Huangheyan    | 4450            | Yellow      | 45015.00                            | 85.50  | 441.48        | -4.16        | 0.26 | 0.61 | 0.00  | 17.25 |
| 11   | Jimai         | 2599            | Yalong      | 67514.00                            | 237.66   | 717.05        | -0.23        | 0.43 | 0.52 | 0.00  | 20.05 |
| 12   | Yajiang       | 3540            | Yangtze     | 137704.00                           | 96.23  | 405.66        | -4.83        | 0.20 | 0.80 | 0.15  | 18.36 |
|  | Zhimenda      |                 |             |                                     |  |               |              |      | 0.26 | 0.96  | 17.87 |
| <i><b>Indian monsoon-dominated basins:</b></i>     |               |                 |             |                                     |  |               |              |      |      |       |       |
|  | Jiaoyuqiao    | 3000            | Salween     | 72844.00                            | 364.26   | 620.88        | -1.89        | 0.29 |      | 2.02  |       |

带格式的: 字体: 倾斜

带格式的: 字体: 加粗, 倾斜

带格式的: 左

带格式的: 字体: 加粗, 倾斜

带格式的: 左

带格式的: 字体: 小四, 加粗, 倾斜, 字体颜色: 文字 1

带格式的: 字体: 倾斜

带格式的: 左

带格式的: 字体: 加粗, 倾斜

849  
850

|               |                    |                 |                        |                      |                   |                   |                  |                 |                 |                 |                  |
|---------------|--------------------|-----------------|------------------------|----------------------|-------------------|-------------------|------------------|-----------------|-----------------|-----------------|------------------|
| 13            | Pangduo            | 5015            | Brahmaputra            | 16459.00             | 348.31            | 544.59            | -1.53            | 0.27            | 0.44            | 1.66            | 23.73            |
| 14            | Tangjia            | 4982            | Brahmaputra            | 20143.00             | 350.61            | 555.17            | -1.89            | 0.27            | 0.33            | 1.39            | 23.33            |
| 15            | Gongbujiangda      | 4927            | Brahmaputra            | 6417.00              | 586.96            | 692.06            | -4.24            | 0.27            | 0.34            | 4.12            | 21.83            |
| 16            | Nuxia              | 2910            | Brahmaputra            | 191235.00            | 307.38            | 401.35            | -0.73            | 0.22            | 0.36            | 1.90            | 25.99            |
| 17            | <u>Yangcun</u>     | <u>3600</u>     | <u>Brahmaputra</u>     | <u>152701.00</u>     | <u>163.25</u>     | <u>349.91</u>     | <u>-0.87</u>     | <u>0.19</u>     | 0.25            | <u>1.28</u>     | 13.50            |
| <u>18</u>     |                    |                 |                        |                      |                   |                   |                  |                 | <u>0.18</u>     |                 | <u>10.52</u>     |
|               | <del>Yangcun</del> | <del>3600</del> |                        | <del>152701.00</del> | <del>163.25</del> | <del>349.91</del> | <del>-0.87</del> | <del>0.19</del> |                 | <del>1.28</del> |                  |
| <del>18</del> |                    |                 | <del>Brahmaputra</del> |                      |                   |                   |                  |                 | <del>0.18</del> |                 | <del>10.52</del> |

851  
852  
853  
854

**Table 3:** Annual-averaged water storage changes ( $\Delta S$ ) in 18 TP basins derived from GRACE retrievals (2002-2013) from three different processing centers (CSR, GFZ and JPL)

| Basin                                      | Water storage Change ( $\Delta S$ ,mm) |                  |                  |
|--|--|------------------|------------------|
|  | CSR                                    | GFZ              | JPL              |
| <i><u>Westerlies-dominated basins:</u></i> | <del>-0.10</del>                       | <del>-0.22</del> | <del>-0.41</del> |
|  | -0.24                                  | -0.35            | -0.41            |
|  | -0.16                                  | 0.35             | 0.15             |
|  | -0.50                                  | 0.38             | -1.13            |
|  | -1.44                                  | -1.29            | -1.46            |
|  | -1.67                                  | -1.34            |                  |

带格式的: 字体颜色: 自动设置

带格式的: 字体: 倾斜

带格式的: 左

|               |       |              |       |
|---------------|-------|--------------|-------|
| Kulukelangan  | -0.16 | <u>-0.16</u> | -0.00 |
| Tongguziluoke | 0.10  | <u>0.10</u>  | 0.28  |
| Numaitilangan | 0.24  | <u>0.22</u>  | 0.41  |

***East Asian monsoon-dominated basins:***

|             |       |              |       |
|-------------|-------|--------------|-------|
| Zelingou    |       | <u>0.41</u>  |       |
| Gadatan     | 0.63  | <u>-0.24</u> | 0.69  |
| Xining      | 0.02  | <u>-0.35</u> | -0.03 |
| Tongren     | -0.08 | <u>-0.41</u> | -0.14 |
| Tainaihai   | -0.13 | <u>-0.16</u> | -0.21 |
| Huangheyang | 0.12  | <u>0.35</u>  | 0.10  |
| Jimai       | 0.60  | <u>0.15</u>  | 0.70  |
| Yajiang     | 0.41  | <u>-0.50</u> | 0.48  |
| Zhimenda    | -0.23 | <u>0.38</u>  | -0.21 |
|             | 0.57  |              | 0.78  |

***Indian monsoon-dominated basins:***

|               |       |              |       |
|---------------|-------|--------------|-------|
| Jiaoyuqiao    |       | <u>-1.13</u> |       |
| Nuxia         | -1.00 | <u>-1.44</u> | -0.79 |
| Pangduo       | -1.42 | <u>-1.29</u> | -1.31 |
| Tangjia       | -1.21 | <u>-1.46</u> | -1.02 |
| Gongbujiangda | -1.40 | <u>-1.67</u> | -1.24 |
| Yangcun       | -1.61 | <u>-1.34</u> | -1.47 |
|               | -1.33 |              | -1.21 |

855

856

857

**Table 4:** Nonparametric trends for different ET estimates

858 during the period 1982-2006 detected by modified Mann-Kendall test, the bold number showed the detected trend is statistically significant at the 0.05 level

带格式的：字体：倾斜

带格式的：左

带格式的：字体：倾斜

带格式的：左

带格式的：字体颜色：自动设置

带格式表格

带格式的: 字体: (默认) +西文正文, 五号

| Basin         | ET <sub>wb</sub> | GLEAM_E     | VIC_E       | Zhang_E      | PML_E       | MET_E        | GNoah_E     |
|---------------|------------------|-------------|-------------|--------------|-------------|--------------|-------------|
| Kulukelangan  | <b>-0.09</b>     | 0.09        | <b>0.18</b> | =            | 0.03        | -0.01        | 0.07        |
| Tongguziluo   | -0.02            | 0.10        | <b>0.13</b> | =            | 0.03        | <b>-0.08</b> | 0.19        |
| Numaitilangan | 0.04             | <b>0.10</b> | 0.14        | =            | 0.14        | <b>-0.10</b> | 0.22        |
| Zelingou      | <b>0.13</b>      | <b>0.23</b> | 0.11        | <b>0.09</b>  | 0.04        | <b>0.06</b>  | 0.02        |
| Gadatan       | -0.09            | 0.25        | 0.070       | -0.10        | -0.01       | <b>0.06</b>  | -0.07       |
| Xining        | -0.06            | <b>0.54</b> | 0.01        | -0.08        | 0.01        | 0.02         | -0.06       |
| Tongren       | -0.06            | <b>0.34</b> | -0.15       | <b>-0.17</b> | 0.07        | 0.02         | 0.13        |
| Tainaihai     | 0.06             | <b>0.28</b> | -0.03       | <b>-0.11</b> | 0.04        | <b>0.05</b>  | 0.04        |
| Huangheyan    | 0.08             | <b>0.19</b> | -0.01       | <b>-0.10</b> | <b>0.08</b> | <b>0.05</b>  | <b>0.10</b> |
| Jimai         | -0.07            | <b>0.23</b> | -0.01       | -0.08        | 0.03        | <b>0.05</b>  | 0.10        |
| Yajiang       | 0.17             | <b>0.26</b> | <b>0.06</b> | <b>-0.21</b> | -0.01       | 0.03         | -0.02       |
| Zhimenda      | 0.11             | <b>0.28</b> | 0.10        | 0.01         | 0.07        | <b>0.04</b>  | 0.07        |
| Jiaoyuqiao    | <b>0.18</b>      | <b>0.28</b> | 0.10        | <b>-0.11</b> | 0.05        | <b>0.05</b>  | 0.07        |
| Nuxia         | <b>-0.09</b>     | <b>0.25</b> | 0.09        | <b>-0.10</b> | <b>0.12</b> | <b>0.04</b>  | 0.10        |
| Pangduo       | 0.05             | <b>0.28</b> | <b>0.17</b> | <b>-0.07</b> | 0.07        | <b>0.07</b>  | <b>0.11</b> |
| Tangjia       | 0.09             | <b>0.26</b> | <b>0.17</b> | <b>-0.09</b> | <b>0.20</b> | <b>0.06</b>  | <b>0.12</b> |
| Gongbujiangda | -0.26            | 0.12        | 0.13        | <b>-0.16</b> | <b>0.19</b> | 0.01         | <b>0.15</b> |
| Yangeun       | 0.03             | <b>0.28</b> | 0.08        | <b>-0.06</b> | 0.10        | 0.04         | 0.09        |

|       |                  |         |       |         |       |       |         |
|-------|------------------|---------|-------|---------|-------|-------|---------|
| Basin | ET <sub>wb</sub> | GLEAM_E | VIC_E | Zhang_E | PML_E | MET_E | GNoah_E |
|-------|------------------|---------|-------|---------|-------|-------|---------|

**Westerlies-dominated basins:**

带格式的: 字体: 倾斜

|     |  |              |             |              |              |              |              |              |
|-----|--|--------------|-------------|--------------|--------------|--------------|--------------|--------------|
| 860 | <u>Kulukelangan</u>                                | <u>-0.09</u> | <u>0.09</u> | <u>0.18</u>  | <u>-</u>     | <u>0.03</u>  | <u>-0.01</u> | <u>0.07</u>  |
| 861 | <u>Tongguziluo</u>                                 | <u>-0.02</u> | <u>0.10</u> | <u>0.13</u>  | <u>-</u>     | <u>0.03</u>  | <u>-0.08</u> | <u>0.19</u>  |
| 862 | <u>Numaitilangan</u>                               | <u>0.04</u>  | <u>0.10</u> | <u>0.14</u>  | <u>-</u>     | <u>0.14</u>  | <u>-0.10</u> | <u>0.22</u>  |
|     | <u><i>East Asian monsoon-dominated basins:</i></u> |              |             |              |              |              |              |              |
| 863 | <u>Zelingou</u>                                    | <u>0.13</u>  | <u>0.23</u> | <u>0.11</u>  | <u>0.09</u>  | <u>0.04</u>  | <u>0.06</u>  | <u>0.02</u>  |
|     | <u>Gadatan</u>                                     | <u>-0.09</u> | <u>0.25</u> | <u>0.070</u> | <u>-0.10</u> | <u>-0.01</u> | <u>0.06</u>  | <u>-0.07</u> |
| 864 | <u>Xining</u>                                      | <u>-0.06</u> | <u>0.54</u> | <u>0.01</u>  | <u>-0.08</u> | <u>0.01</u>  | <u>0.02</u>  | <u>-0.06</u> |
|     | <u>Tongren</u>                                     | <u>-0.06</u> | <u>0.34</u> | <u>-0.15</u> | <u>-0.17</u> | <u>0.07</u>  | <u>0.02</u>  | <u>0.13</u>  |
| 865 | <u>Tainaihai</u>                                   | <u>0.06</u>  | <u>0.28</u> | <u>-0.03</u> | <u>-0.11</u> | <u>0.04</u>  | <u>0.05</u>  | <u>0.04</u>  |
|     | <u>Huangheyan</u>                                  | <u>0.08</u>  | <u>0.19</u> | <u>-0.01</u> | <u>-0.10</u> | <u>0.08</u>  | <u>0.05</u>  | <u>0.10</u>  |
| 866 | <u>Jimai</u>                                       | <u>-0.07</u> | <u>0.23</u> | <u>-0.01</u> | <u>-0.08</u> | <u>0.03</u>  | <u>0.05</u>  | <u>0.10</u>  |
|     | <u>Yajiang</u>                                     | <u>0.17</u>  | <u>0.26</u> | <u>0.06</u>  | <u>-0.21</u> | <u>-0.01</u> | <u>0.03</u>  | <u>-0.02</u> |
| 867 | <u>Zhimenda</u>                                    | <u>0.11</u>  | <u>0.28</u> | <u>0.10</u>  | <u>0.01</u>  | <u>0.07</u>  | <u>0.04</u>  | <u>0.07</u>  |
|     | <u><i>Indian monsoon-dominated basins:</i></u>     |              |             |              |              |              |              |              |
| 868 | <u>Jiaoyuqiao</u>                                  | <u>0.18</u>  | <u>0.28</u> | <u>0.10</u>  | <u>-0.11</u> | <u>0.05</u>  | <u>0.05</u>  | <u>0.07</u>  |
|     | <u>Nuxia</u>                                       | <u>-0.09</u> | <u>0.25</u> | <u>0.09</u>  | <u>-0.10</u> | <u>0.12</u>  | <u>0.04</u>  | <u>0.10</u>  |
| 869 | <u>Pangduo</u>                                     | <u>0.05</u>  | <u>0.28</u> | <u>0.17</u>  | <u>-0.07</u> | <u>0.07</u>  | <u>0.07</u>  | <u>0.11</u>  |
|     | <u>Tangjia</u>                                     | <u>0.09</u>  | <u>0.26</u> | <u>0.17</u>  | <u>-0.09</u> | <u>0.20</u>  | <u>0.06</u>  | <u>0.12</u>  |
| 870 | <u>Gongbujiangda</u>                               | <u>-0.26</u> | <u>0.12</u> | <u>0.13</u>  | <u>-0.16</u> | <u>0.19</u>  | <u>0.01</u>  | <u>0.15</u>  |
|     | <u>Yangcun</u>                                     | <u>0.03</u>  | <u>0.28</u> | <u>0.08</u>  | <u>-0.06</u> | <u>0.10</u>  | <u>0.04</u>  | <u>0.09</u>  |

带格式的: 字体: 倾斜

带格式的: 字体: 倾斜

**Figure captions:**

**Figure1.** Map of river basins and hydrological gauging stations (green dots) over the Tibetan Plateau (TP) used in this study. The grey shading shows the topography of TP in meters above the sea level and the blue shading exhibits the glaciers distribution in TP extracted from the Second Glacier Inventory Dataset of China.

**Figure 2.** Comparison of VIC\_IGSNRR simulated and observed monthly runoff for Tangnaihai and Panduo stations (a and b) as well as (c) basin-averaged monthly TRMM, CMA gridded and IGSNRR forcing precipitations for the smallest basin (Tongren station) over the period 1982-2011. (d) shows the comparison of TRMM (blue) and IGSNRR forcing (red) precipitations against CMA gridded precipitation for 18 river basins over TP during the period 2000-2011.

**Figure 3.** Comparison of different ET products against the calculated ET through the water balance method ( $ET_{wb}$ ) at the monthly time scale for 18 TP basins during the period 1983-2006. The boxplot of monthly estimates of different ET products for 18 TP basins are shown in (a) while the correlation coefficients and root-mean-square-errors (RMSEs, mm/month) for each ET product relatively to  $ET_{wb}$  are exhibited in (b).

**Figure 4.** General water and energy status (a. the perspective of Budyko framework) and their relationships with glacier (b) and vegetation (c and d) for eighteen TP river basins (1983-2006). The ET used in this figure is calculated from the bias-corrected water balance method.

**Figure 5.** Seasonal cycles (1982-2011) of water budget components in westerlies-dominated (column 1), East Asian monsoon-dominated (columns 2-4) and Indian monsoon-dominated (columns 5-6) TP basins.

**Figure 6.** Seasonal cycles (1982-2011) of air temperature and vegetation parameters in westerlies-dominated (column 1), East Asian monsoon-dominated (columns 2-4) and Indian monsoon-dominated (columns 5-6) TP basins.

**Figure 7.** Seasonal cycles (1982-2011) of snow cover and snow water equivalent (SWE) in westerlies-dominated (column 1), East Asian monsoon-dominated (columns



2-4) and Indian monsoon-dominated (columns 5-6) TP basins. The snow cover was extracted from cloud free snow composite product during the period 2005-2013. It should also be noted that the GlobSnow data are not available for some basins.

**Figure 8.** Sen's slopes of water budget components and vegetation parameters in westerlies-dominated TP basins during the period of 1982-2011. To clearly exhibit the nonparametric trends of all variables in one panel, the Sen's Slopes of Q, P,  $ET_{wb}$  and PET have been multiplied by 1/12 (unit: mm/month). The double red stars showed that the trend was statistically significant at the 0.05 level.

**Figure 9.** Linear and non-parametric trends of westerly, Indian monsoon and East Asian summer monsoon during the period 1982-2011 revealed prospectively by the Asian Zonal Circulation Index, Indian Ocean Dipole Mode Index and East Asian Summer Monsoon Index.

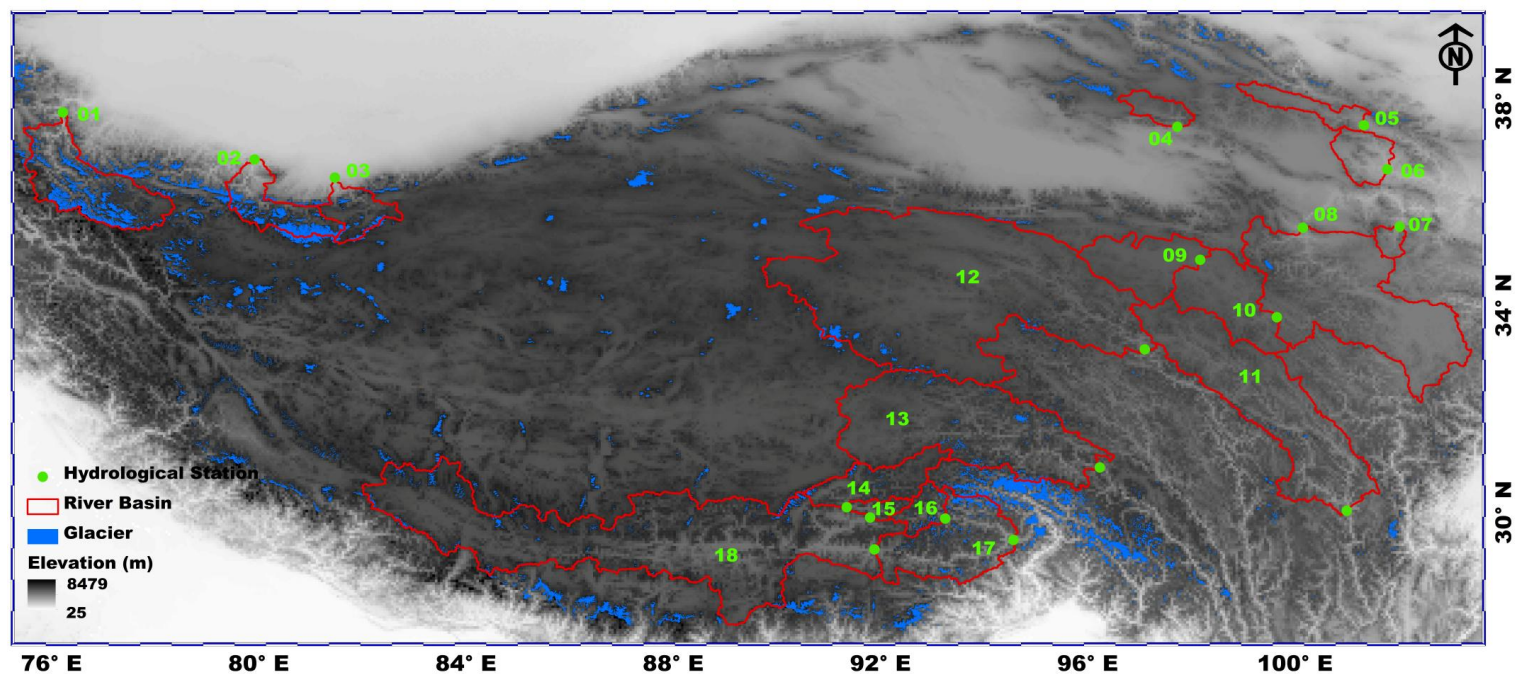
**Figure 10.** Similar to Figure 8 but for East Asian monsoon-dominated TP basins. It should be noted that the GlobSnow data are not available for some basins. The double red stars showed that the trend was statistically significant at the 0.05 level.

**Figure 11.** Similar to Figure 8 but for Indian monsoon-dominated TP basins. It should be noted that the GlobSnow data are not available for some basins. The double red stars showed that the trend was statistically significant at the 0.05 level.

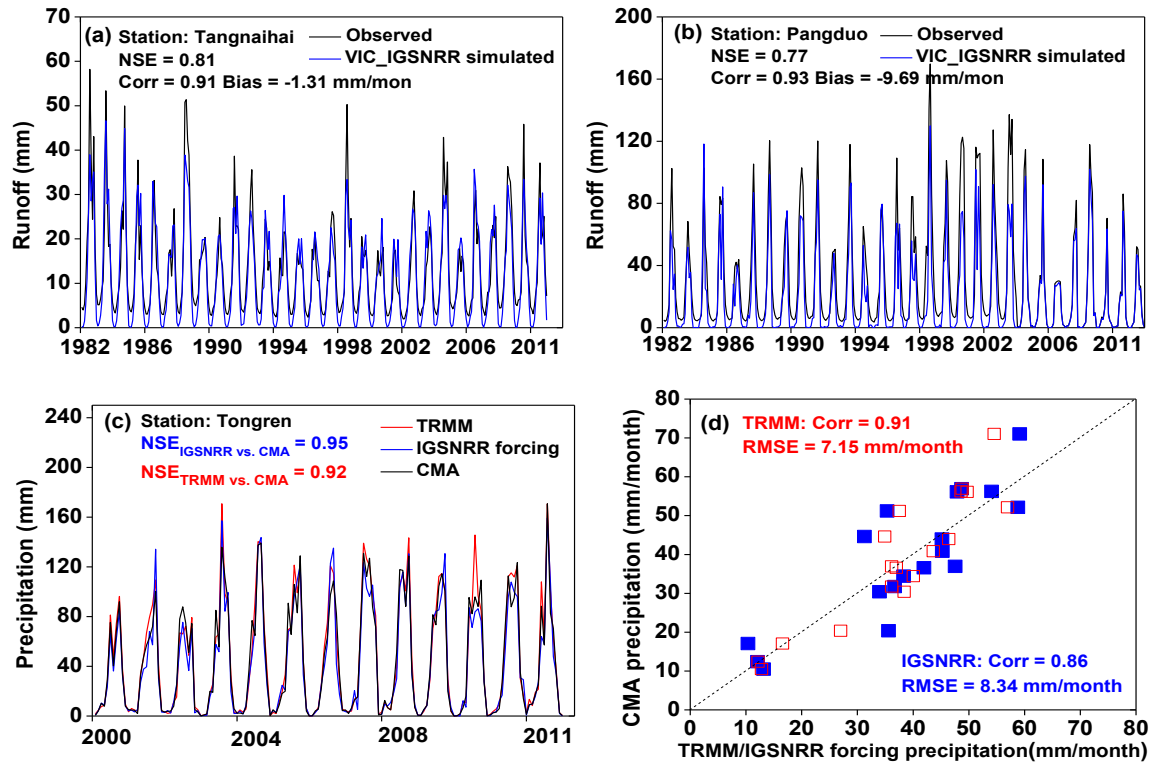
**Figure 12.** Uncertainties in seasonal cycles of  $ET_{wb}$  calculated from three precipitation products (CMA gridded, IGSNRR\_Forcing and TRMM precipitation) in 18 TP basins. The comparisons were conducted during the period 2000-2011 when TRMM data was available.

**Figure 13.** Uncertainties in annual trends of  $ET_{wb}$  (b) calculated from two precipitation products (CMA gridded and IGSNRR\_Forcing) (a) in 18 TP basins. The comparisons were conducted during the period 1982-2011 (TRMM data was not available for the whole period).

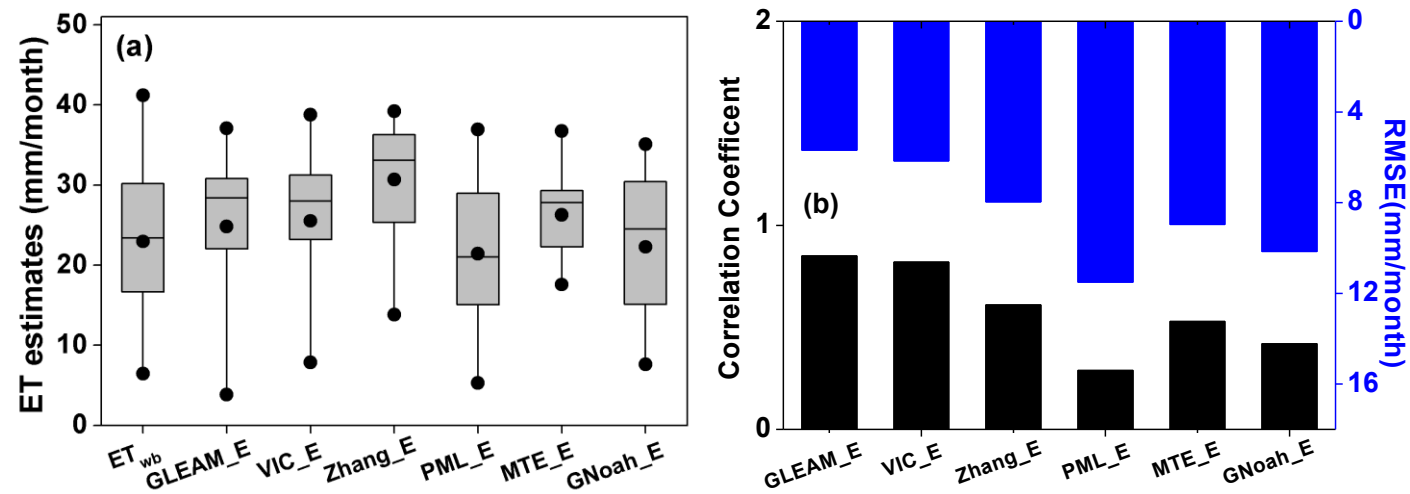
928 **Figure 1.** Map of river basins and hydrological gauging stations (green dots) over the Tibetan Plateau (TP) used in this study. The grey shading shows the  
929 topography of TP in meters above the sea level and the blue shading exhibits the glaciers distribution in TP extracted from the Second Glacier Inventory Dataset of  
930 China.



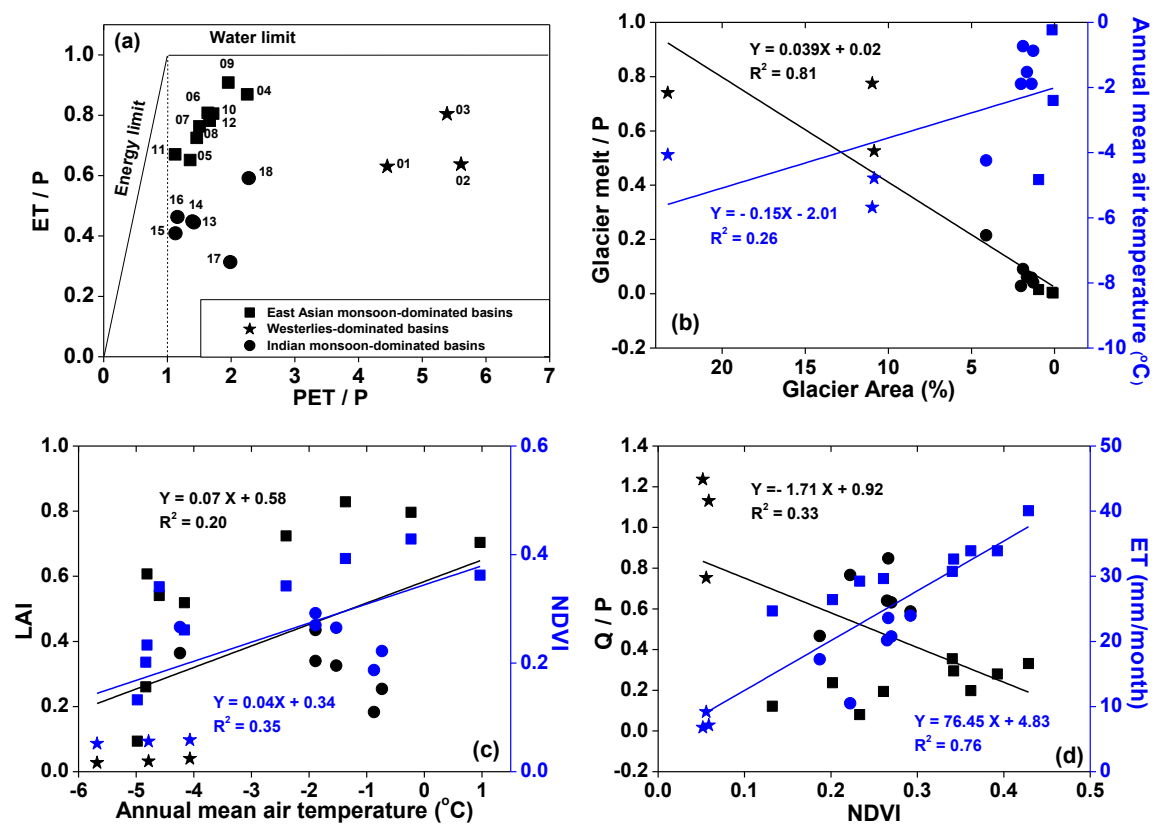
933 **Figure 2.** Comparison of VIC\_IGSNRR simulated and observed monthly runoff for Tangnaihui and Panduo stations (a and b) as well as (c) basin-averaged  
 934 monthly TRMM, CMA gridded and IGSNRR forcing precipitations for the smallest basin (Tongren station) over the period 1982-2011. (d) shows the comparison of  
 935 TRMM (blue) and IGSNRR forcing (red) precipitations against CMA gridded precipitation for 18 river basins over TP during the period 2000-2011.



939 **Figure 3.** Comparison of different ET products against the calculated ET through the water balance ( $ET_{wb}$ ) at the monthly time scale for 18 river basins over the  
 940 Tibetan Plateau during the period 1983-2006. The boxplot of monthly estimates of different ET products for 18 TP basins are shown in (a) while the correlation  
 941 coefficients and root-mean-square-errors (RMSEs, mm/month) for each ET product relatively to  $ET_{wb}$  are exhibited in (b).



944 **Figure 4.** General water and energy status (a. the perspective of Budyko framework) and their relationships with glacier (b) and vegetation (c and d) for eighteen  
945 TP river basins (1983-2006). The ET used in this figure is calculated from the bias-corrected water balance method.

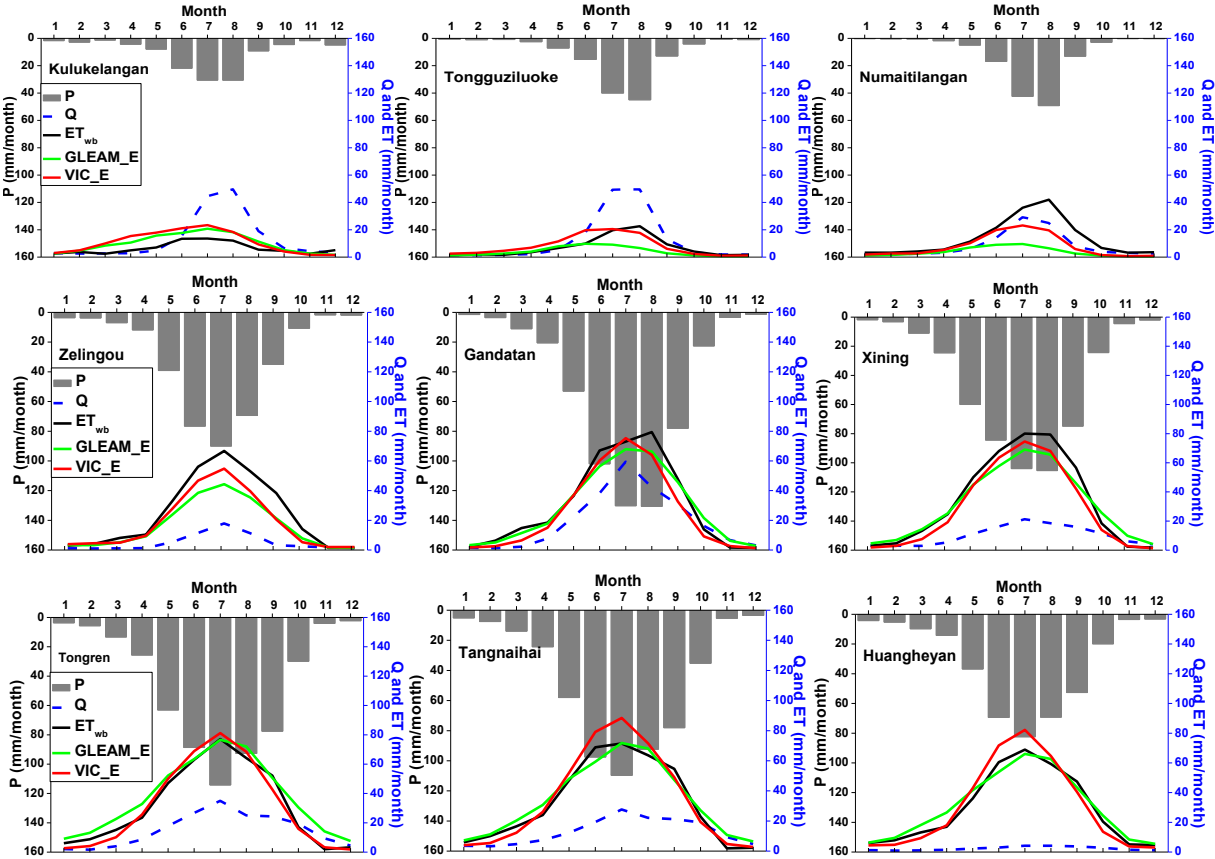


948 **Figure 5.** Seasonal cycles (1982-2011) of water budget components in westerlies-dominated (column 1), East Asian monsoon-dominated (columns 2-4) and Indian  
 949 monsoon-dominated (columns 5-6) TP basins.

950

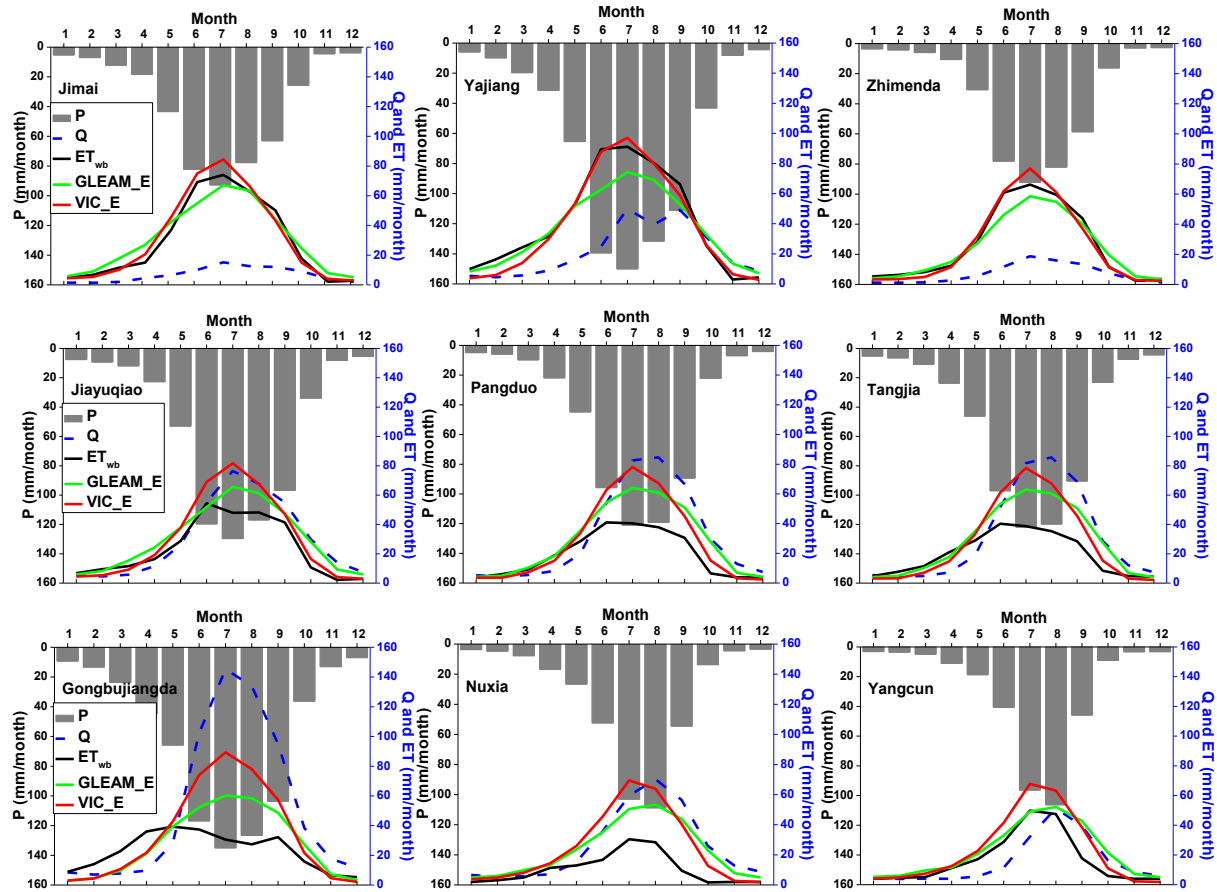
951

952



953

Figure 5: (continued)

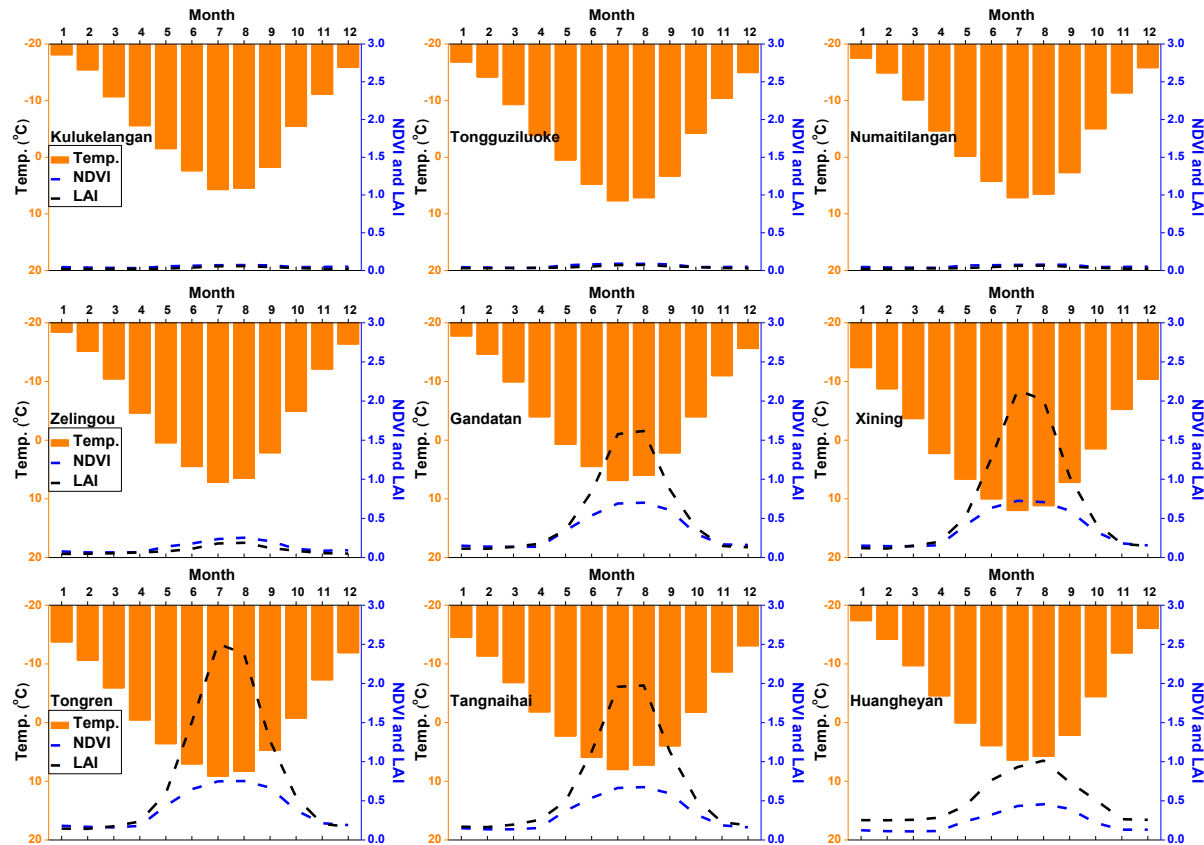


954

955

956

957 **Figure 6.** Seasonal cycles (1982-2011) of air temperature and vegetation parameters in westerlies-dominated (column 1), East Asian monsoon-dominated (columns  
958 2-4) and Indian monsoon-dominated (columns 5-6) TP basins.





962

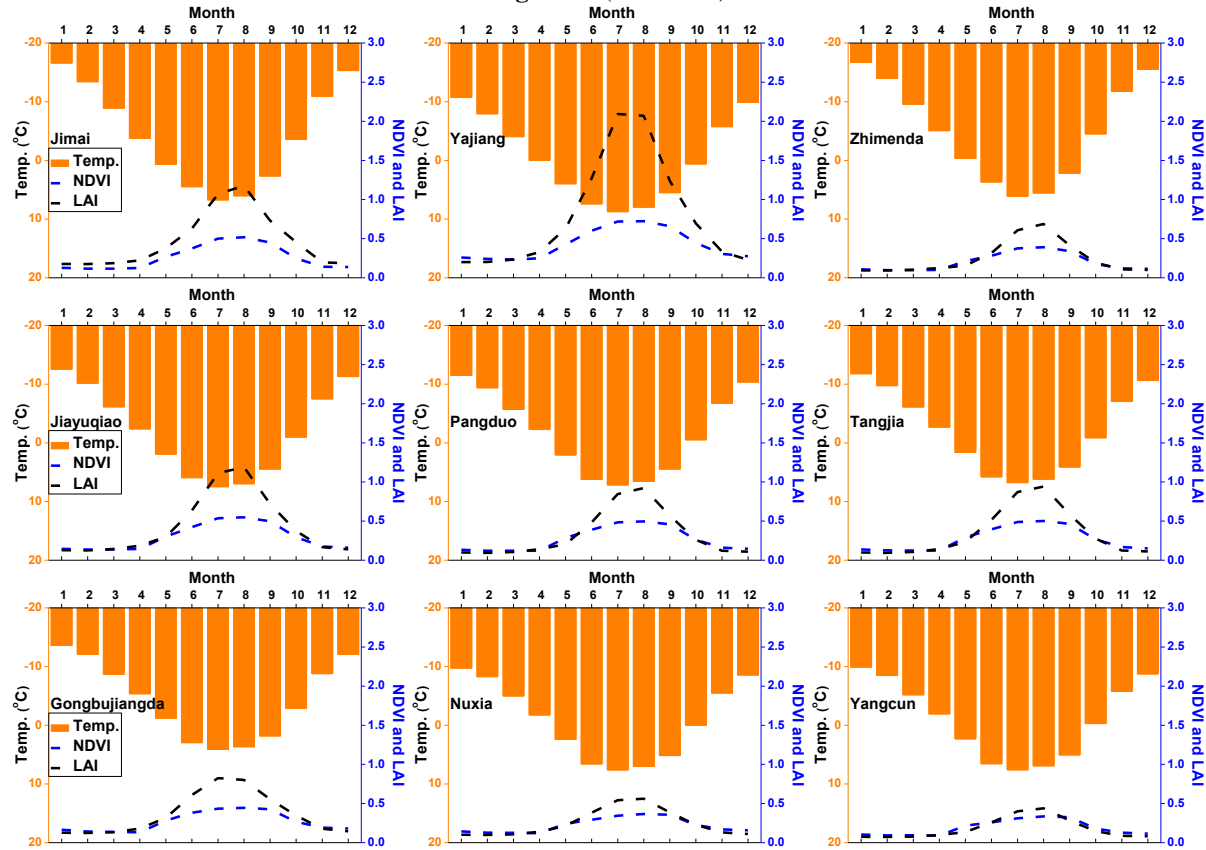
963

964

965

966

Figure 6: (continued)



967 **Figure 7.** Seasonal cycles (1982-2011) of snow cover and snow water equivalent (SWE) in westerlies-dominated (column 1), East Asian monsoon- dominated  
968 (columns 2-4) and Indian monsoon-dominated (columns 5-6) TP basins. The snow cover was extracted from cloud free snow composite product during the period  
969 2005-2013. It should also be noted that the GlobSnow data are not available for some basins.  
970

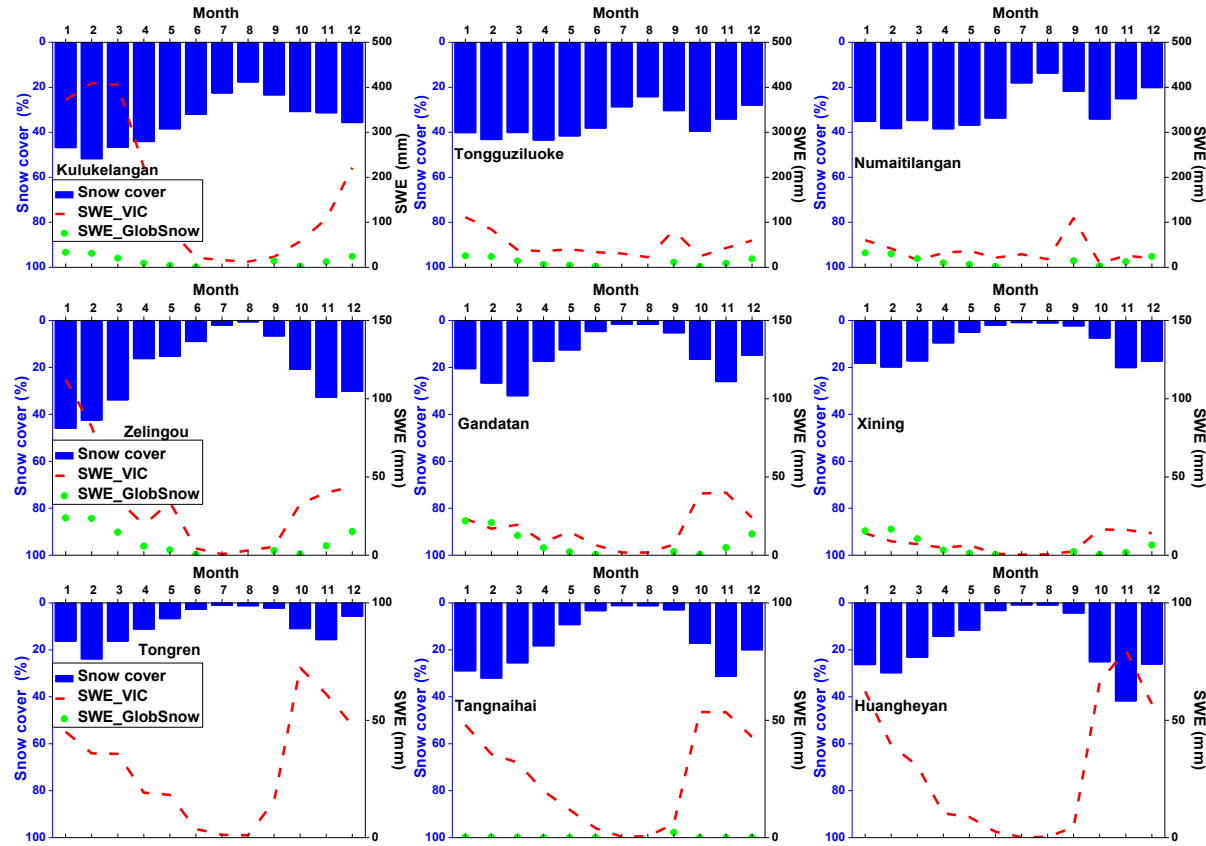
971

972

973

974

975



976

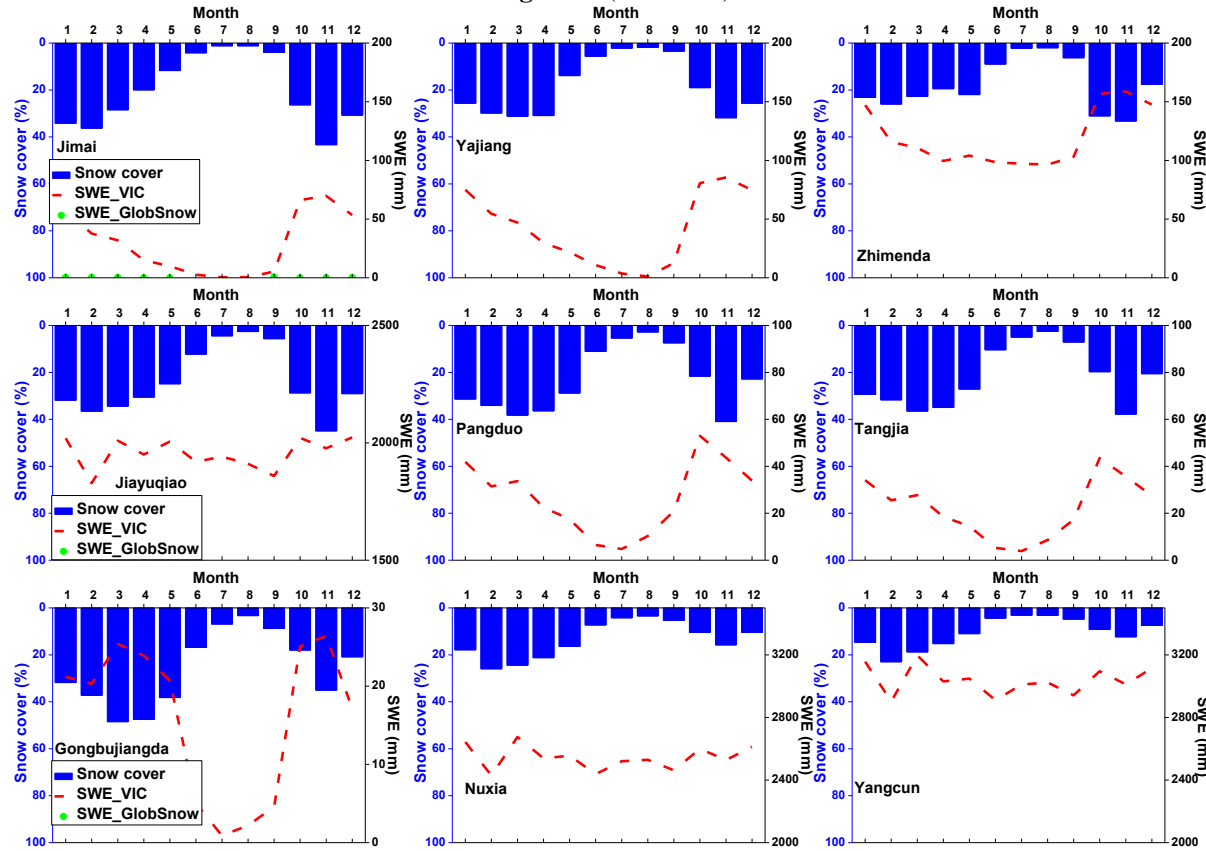
977

978

979

980

Figure 7: (continued)



981 **Figure 8.** Sen's slopes of water budget components and vegetation parameters in westerlies-dominated TP basins during the period of 1982-2011. To clearly  
 982 exhibit the nonparametric trends of all variables in one panel, the Sen's Slopes of Q, P, ET<sub>wb</sub> and PET have been multiplied by 1/12 (unit: mm/month). The double  
 983 red stars showed that the trend was statistically significant at the 0.05 level.

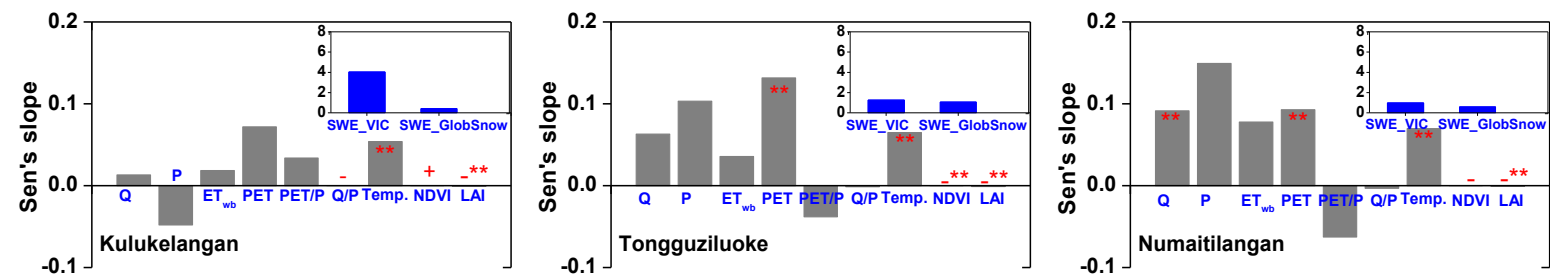
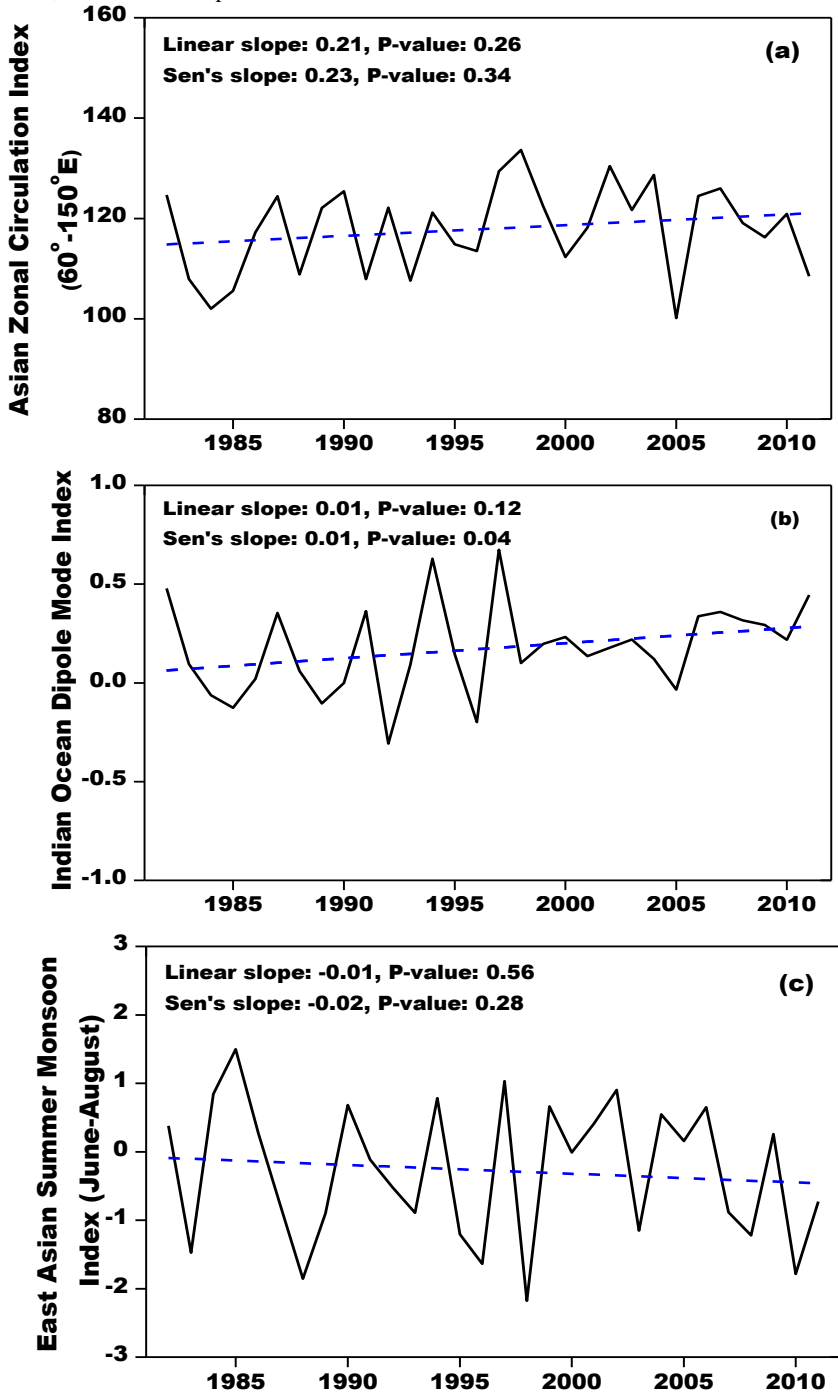
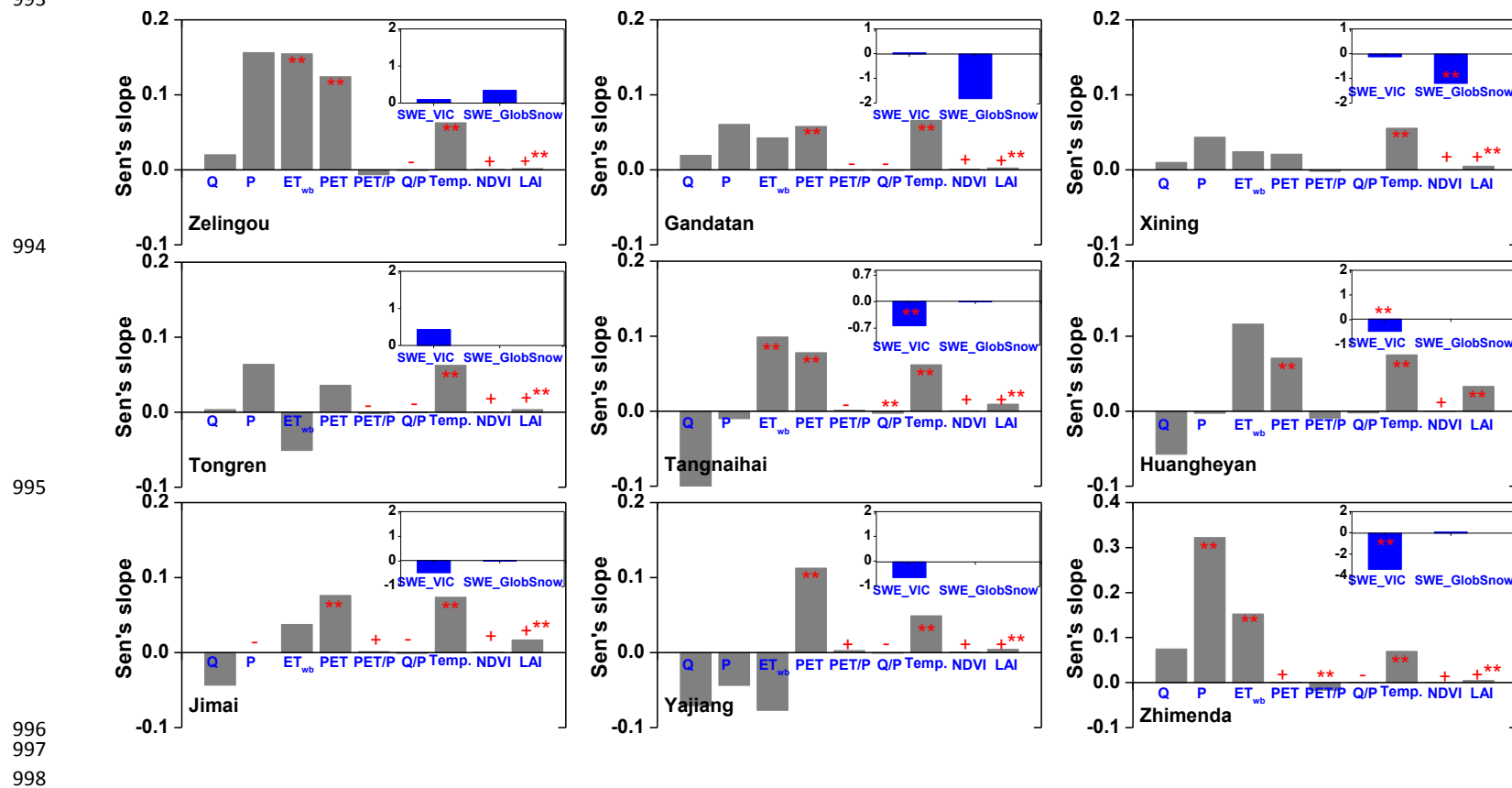


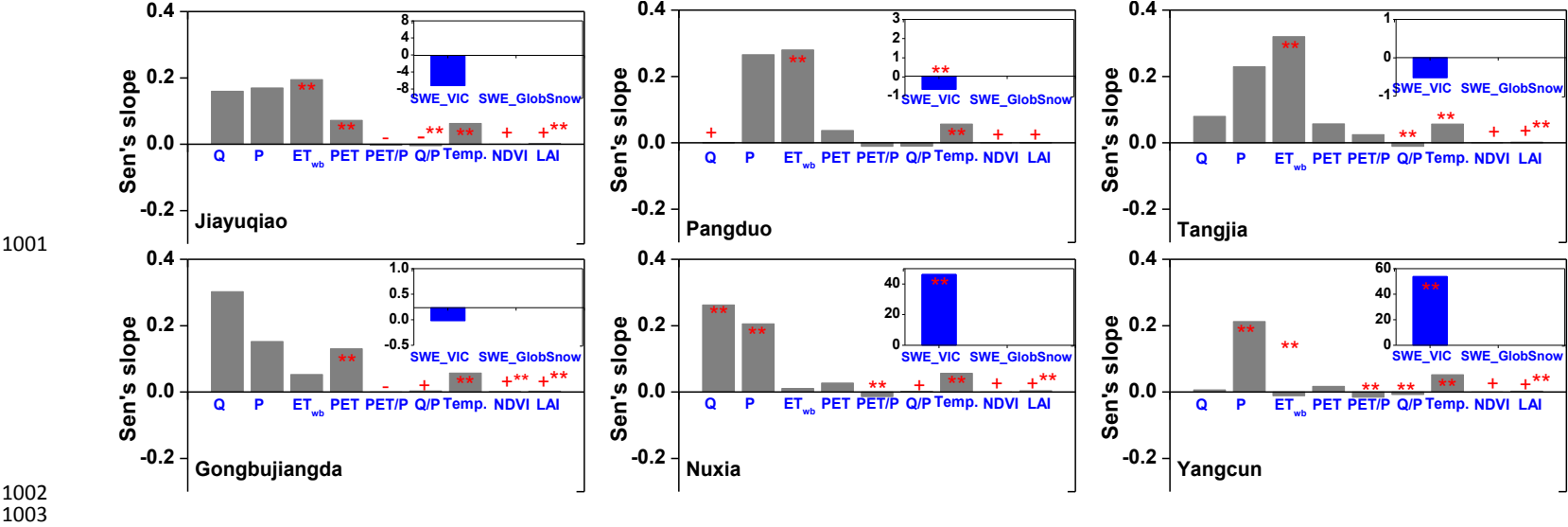
**Figure 9.** Linear and non-parametric trends of westerly, Indian monsoon and East Asian summer monsoon during the period 1982-2011 revealed prospectively by the Asian Zonal Circulation Index, Indian Ocean Dipole Mode Index and East Asian Summer Monsoon Index.



992 **Figure 10.** Similar to Figure 8 but for East Asian monsoon-dominated TP basins. It should be noted that the GlobSnow data are not available for some basins.  
993

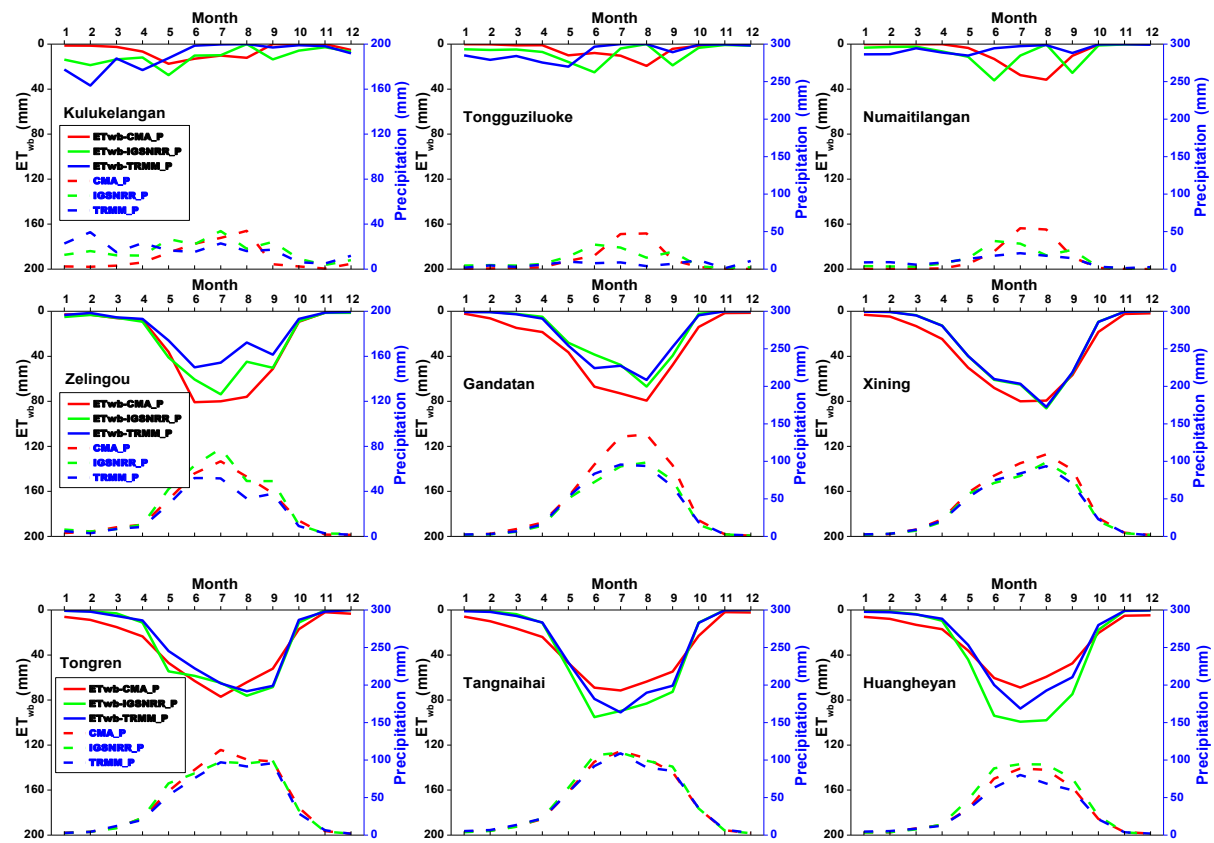


999 **Figure 11.** Similar to Figure 8 but for Indian monsoon-dominated TP basins. It should be noted that the GlobSnow data are not available for some basins.  
1000





1004 **Figure 12.** Uncertainties in seasonal cycles of  $ET_{wb}$  calculated from three precipitation products (CMA gridded, IGSNRR\_Forcings and TRMM precipitation) in 18 TP  
1005 basins. The comparisons were conducted during the period 2000-2011 when TRMM data was available.



1010

1011

1012

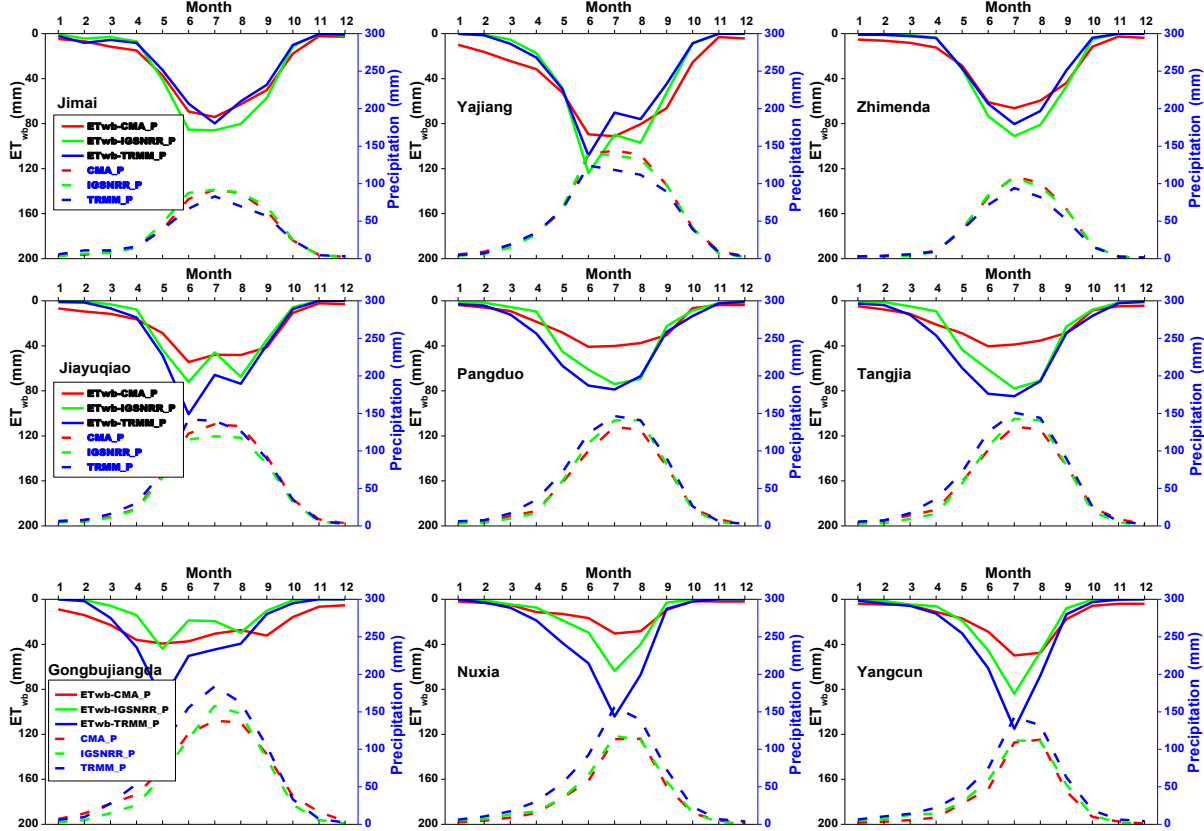
1013

1014

1015

1016

Figure 12: (continued)



1017 **Figure 13.** Uncertainties in annual trends of  $ET_{wb}$  (b) calculated from two precipitation products (CMA gridded and IGSNRR\_Fforcing) (a) in 18 TP basins. The  
1018 comparisons were conducted during the period 1982-2011(TRMM data was not available for the whole period).

